The Evolution of Live Birth and the Insulin and Insulin-like Signaling Network in *Sceloporus* Lizards

By

Aundrea Kristene Westfall

A thesis submitted to the Graduate Faculty of
Auburn University
in partial fulfillment of the
requirements for the Degree of
Master of Science

Auburn, Alabama
August 4th, 2018

Keywords: *Sceloporus undulatus*, comparative genomics, molecular evolution, Dollo's law, cold climate hypothesis, convergence

Approved by

Tonia S. Schwartz, Assistant Professor of Biological Sciences
Jamie R. Oaks, Assistant Professor of Biological Sciences
Wendy R. Hood, Associate Professor of Biological Sciences

Abstract

Transitions to live birth have occurred in approximately 150 different vertebrate lineages, with 115 of these alone within the clade encompassing snakes and lizards. Many questions remain about how this transition occurs and how molecular networks are evolving associated with the new character state, including the insulin and insulin-like signaling (IIS) network, which fills major roles in structuring and maintain the mammalian placenta. The genus *Sceloporus* is made up of over 100 species and includes three major groups of live bearing lizards. The recent publication of genomic data for 33 of these species makes them an ideal model to begin investigating the evolution of the IIS network, focusing on two major features: differences in substitution rate in these genes between viviparous and oviparous species, and positive selection within viviparous groups. We provide evidence for widespread increases in substitution rates across genes in this network in viviparous lineages and more limited evidence of positive selection in genes which have major functions related to angiogenesis, tissue proliferation, and oncogenesis.

Acknowledgements

I would like to thank my co-advisors Drs. Tonia Schwartz and Jamie Oaks for their continuous, unwavering support; their faith in my capabilities; and for always pushing me to the produce the best possible work that I can. Thank you for providing the opportunities in your labs at Auburn University that have helped me grow as a scientist, a student, and a person. I have learned so much more than I ever expected to under your guidance. I would also like to thank Dr. Wendy Hood for her participation on my committee and for being the reminder I needed that I was not studying just strings of letters on a computer screen but also the animals they came from. I would like to thank my labmates who have for two years put up with my constant and occasionally unintelligible rambling and ranting about genomes, statistics, ovoviviparity, and more, and who have supported me, encouraged me, and helped me through harder obstacles in my work. I would like to thank my parents, Allan and Marrianne Westfall, and my brothers, Allan and Aaron, for everything they have done to help me over these last two years; I would not be here without all they've done for me throughout the course of my life. I would like to thank my closest friends from my time at Auburn: Ariel Steele, Abby Beatty, Chase Rushton, Zach Nikolakis, Tom Witt, and Kayla Wilson. You each know what you've done for me. Finally, I would like to thank my dogs Piper and Jamie (RIP), for being a constant source of comfort and companionship.

Table of Contents

List of Tables

Chapter 1

List of Figures

Introduction

Chapter 1

The Evolution of Viviparity in Reptiles: A Thesis Overview

The evolution of live birth, viviparity, is one of many major topics pressing animal biologists. Transitioning from egg-laying to live-bearing drives questions that cross a number of sub-fields of biology: how does this happen genetically? Physiologically? What in the environment selects for this change, and how? What consequences or trade-offs does this have for the mother? When a lineage becomes viviparous, mothers no longer lay eggs that develop solely under the signals received from the environment. Rather, the maternal metabolism interacts with developing embryos to translate these environmental signals, and new relationships form between mother and fetus which are osmoregulatory, endocrinological, and immunological, among others. Taking into consideration the wide diversity of organisms that have become viviparous (many invertebrates and lineages in almost every major clade of vertebrates) this trait also contributes to conversations on more broad, theoretical concepts in evolution such as convergence and constraint (Wourms 1981; Wake 1993; Blackburn 2015; Wake 2015).

Viviparity is widespread among invertebrate groups, including Platyhelminthes, Nemertea, Annelida, and Insecta, and has evolved in approximately 140 lineages which include thousands of species (Kaye et al. 1972; Ostrovsky et al. 2016). Vertebrate groups, while significantly less speciose, have experienced approximately 150 transitions to live birth, including the most well-known and well-studied, the evolution of viviparity in mammals. The majority of these lineages are in squamates, the group consisting of lizards and snakes, which include over 100 putative transitions to live birth, although the exact number is difficult to ascertain because of the vast number of uncharacterized reproductive modes among squamates as well as contention in the higher order systematics of the group (Blackburn 2015). The

evolutionary pathway between egg-laying, also called oviparity, and viviparity is largely unknown, particularly in amniotes, where the transition requires a series of specific steps involving retention of the egg, loss of the eggshell, suppression of the maternal immune system to prevent spontaneous abortion, and development of communication and exchange at the maternal-fetal interface. While intermediate stages between oviparity and viviparity may exist, none have yet been identified, and it is likely not an evolutionary stable state (Blackburn 1995).

Live birth can provide a number of benefits to offspring, including improved thermoregulation and protection of young (Shine 1995; Blackburn and Stewart 2016), but it can also come at a cost, such as higher maternal energy requirements (Birchard et al. 1984; Beuchat and Vleck 1990; Robert and Thompson 2000). One scorpion species was found to be slower when pregnant, with the majority of females no longer choosing to run from predators; instead, they assume a defensive posture (Shaffer and Formanowicz 1996). Comparisons between oviparous and viviparous fishes found a trade-off in which the viviparous fish stocks had reduced reproductive effort, reduced age of maturity, and lower mortality compared to the oviparous fishes (Gunderson 1997). A viviparous skink species was found to have a significant trade-off between reproductive investment and tail regrowth following autotomy, in which the timing of the tail loss significantly affected litter size and offspring size at birth (Chapple et al. 2002). One researcher even proposed that changes in immune system response and regulation in viviparous vertebrates also led to a higher incidence of malignancies than are observed in invertebrates (Hayakawa 2006).

Within reptiles, the vast majority of viviparous species, including all extant viviparous species, are squamates. Twenty six extinct viviparous reptiles have been identified, three of which are placed within squamates, and almost all of which are associated with aquatic habitats,

such as the well-known mosasaurs and plesiosaurs. However, despite their diverse presence in aquatic environments, there have been no identified viviparous turtles or archosaurs, the group including crocodilians, dinosaurs, pterosaurs, and birds. Given the apparent lability of parity mode in squamates, other reptile lineages may be under a specific constraint preventing a transition to live birth; some hypothesize this may have even contributed to the extinction of dinosaurs when they struggled to compete with mammals during their post-K-T diversification (Codron et al. 2012; Blackburn and Sidor 2014).

The Insulin and Insulin-like Signaling Network

The insulin and insulin-like signaling (IIS) network plays a vital role in a number of physiological processes, including fetal growth and development (Irving and Lala 1995; Laviola et al. 2005), aging (Kenyon 2010), life-history plasticity (Dantzer and Swanson 2012), body size (Sutter et al. 2007; Greer et al. 2011), and cognition (Messier and Teutenberg 2005; Tong et al. 2009; Talbot et al. 2012). Research has demonstrated the importance of the IIS network in mammalian viviparity, as it is crucial to the development, function, and maintenance of the placenta, and dysregulation of this molecular network during fetal growth can have dramatic and often deleterious effects on the organism (Laviola et al. 2005; Forbes and Westwood 2008). Top regulators of the IIS network are insulin-like growth factors (IGF1 and IGF2), insulin (INS), their receptors (INSR, IGF1R, and IGF2R), and IGF binding proteins (IGFBP-1 through -7). These activate and interact with downstream nodes in the network to influence phosphoinositide-3 kinase (PI3K)-protein kinase B (AKT), mitogen-activated protein kinase (MAPK), mechanistic target of rapamycin (mTOR), and G-protein-coupled signaling pathways. In mammals, both the maternal and fetal IIS network function together to regulate many cellular functions, including

trophoblast proliferation, migration, and apoptosis; differentiation and vascularization of placental tissues; nutrient utilization and transport; and hormone synthesis (Hiden et al. 2006; Sferruzzi-Perri et al. 2017).

While the vast majority of IIS network research has focused on mammalian and invertebrate systems, a few researchers have recently turned their attention toward reptiles, primarily investigating evolution in the IIS pathway related to environmental stress and life history tradeoffs (Schwartz and Bronikowski 2011; Schwartz and Bronikowski 2014; Duncan et al. 2015; Reding et al. 2016; Addis et al. 2017). In reptiles, extracellular genes in the IIS network (IGFs, their receptors, and IGFBPs) exhibit faster evolutionary rates than the rest of the genome and include many genes under positive selection, such as IGF1, IGF1R, and IGF2R (Sparkman et al. 2012; McGaugh et al. 2015). However, other genes that are under strong positive selection in mammals are highly conserved in reptiles, such as the hormone IGF2 (McGaugh et al. 2015).

Study Organism

Lizards of the genus *Sceloporus* offer a particularly promising model to investigate origins of viviparity. They are a widespread group of approximately 100 species with a well- resolved phylogeny (Leaché et al. 2016) and have between four and six transitions to viviparity, as well as potential transitions back to oviparity. The genus has long been used as a cold-climate model of viviparity evolution, as many viviparous species occur at higher elevations. However, we see the opposite trend in latitude; there are only viviparous species throughout Central America and the southern United States of America, and no extant species of *Sceloporus* has evolved viviparity in higher latitudes. These viviparous species almost all gestate during winter months, and the colder winters in temperate regions may limit range expansion of viviparous species into higher

latitudes or constrain transitions to viviparity (Cruz et al. 1998). The evolution of viviparity in phrynosomatid lizards, including *Sceloporus*, has been associated with an increased rate of evolution in morphological traits, such as in the pelvic girdle and forelimbs, and increased lineage diversification (Oufiero and Gartner 2014), but it also has been demonstrated to decrease variation in life history traits such as offspring size and relative mass, age and size at maturity, and longevity (Zúñiga-Vega et al. 2016). The Genomic Resources Development Consortium et al. (2014, Appendix S2) recently published genomic resources for 35 species in the *Sceloporus* genus, including at least one species from each potential origin of viviparity. One species, *Sceloporus occidentalis*, was sequenced using a shotgun sequencing approach, and sequencing efforts for the 34 remaining species targeted coding regions of the DNA using a reduced representation approach. However, these partial genomes have low coverage and poor quality assemblies with sparse annotation. The eastern fence lizard (*Sceloporus undulatus*) genome was recently sequenced and assembled to near chromosome-level scaffolds; it is the highest quality squamate genome to date.

Thesis Objectives

This thesis leverages multiple independent origins of viviparity in the squamate genus *Sceloporus* to investigate the relationship between live birth and evolution in the IIS network. I seek to address two primary questions: (1) to what extent is there genetic and amino acid variation in the IIS network among *Sceloporus*, and (2) in the IIS genes, are patterns of molecular evolution associated with transitions between oviparity and viviparity? If the IIS network genes are involved in the evolution of viviparity, I hypothesize to find increased rates of evolution in IIS genes on branches with origins of viviparity as well as genes with sites under

positive selection. Finally, this thesis will make a significant contribution of one high coverage, chromosome-level genome assembly and 34 low coverage genomes to the limited pool of squamate genomic resources.

Significance of this Research

One of the most immediate impacts of this thesis are the 35 squamate genomes and their annotations for use in comparative molecular analyses beyond investigations of the evolution of viviparity. This will be the first approach to investigate the evolution of viviparity in squamates by analyzing sequence evolution throughout an entire gene network across a genus, rather than comparative gene expression over just a handful of distantly related species. The repeated evolution of viviparity is a long standing question in evolutionary biology, and uncovering some the mechanisms behind these transitions contributes to our understanding of the evolution of terrestrial eggs, placentation, and placentotrophy. When considered within the context of mammalian viviparity, these results can also contribute to broader questions about homoplasy and homology, exaptation, evolutionary constrains, and selection pressures. Finally, understanding a gene network's evolution from a phylogenetic framework improves our estimation of its history and ancestral state, giving power to future analyses of these genes and the proteins they produce even in other systems.

Literature Cited

Addis EA, Gangloff EJ, Palacios MG, Carr KE, Bronikowski AM. 2017. Merging the "morphology-performance-fitness" paradigm and life-history theory in the eagle lake garter snake research project. Integr. Comp. Biol. 57:423–435.

Beuchat CA, Vleck D. 1990. Metabolic consequences of viviparity in a lizard, Sceloporus jarrovi. Physiol. Zool. 63:555–570.

Birchard GF, Black CP, Schuett GW, Black V. 1984. Influence of pregnancy on oxygen consumption, heart rate and hematology in the garter snake: Implications for the "cost of reproduction" in live bearing reptiles. Comp. Biochem. Physiol. 77A:519–523.

Blackburn DG. 1995. Saltationist and punctuated equilibrium models for the evolution of viviparity and placentation. J. Theor. Biol. 174:199–216.

Blackburn DG. 2015. Evolution of vertebrate viviparity and specializations for fetal nutrition: A quantitative and qualitative analysis. J. Morphol. 276:961–990.

Blackburn DG, Sidor CA. 2014. Evolution of viviparous reproduction in Paleozoic and Mesozoic reptiles. Int. J. Dev. Biol. 58:935–948.

Blackburn DG, Stewart JR. 2016. Viviparity and Placentation in Snakes. In: Aldridge RD, Sever DM, editors. Reproductive Biology and Phylogeny of Snakes. Boca Raton: CRC Press.

Chapple DG, Mccoull CJ, Swain R. 2002. Changes in Reproductive Investment following Caudal Autotomy in Viviparous Skinks (Niveoscincus metallicus): Lipid Depletion or Energetic Diversion? J. Herpetol. 36:480–486.

Codron D, Carbone C, Müller DWH, Clauss M. 2012. Ontogenetic niche shifts in dinosaurs influenced size, diversity and extinction in terrestrial vertebrates. Biol. Lett. 8:620–623.

Cruz FR. M la, Cruz MV-S, Andrews RM. 1998. Evolution of Viviparity in the Lizard Genus Sceloporus. Herpetologica 54:521–532.

Dantzer B, Swanson EM. 2012. Mediation of vertebrate life histories via insulin-like growth factor-1. Biol. Rev. 87:414–429.

Duncan CA, Jetzt AE, Cohick WS, John-Alder HB. 2015. Nutritional modulation of IGF-1 in relation to growth and body condition in Sceloporus lizards. Gen. Comp. Endocrinol. 216:116–124.

Forbes K, Westwood M. 2008. The IGF axis and placental function: A mini review. Horm. Res. 69:129–137.

Genomic Resources Development Consortium, Arthofer W, Banbury BL, Carneiro M, Cicconardi F, Duda TF, Nolte V, Nourisson C, Harris RB, Kang DS, et al. 2014. Genomic Resources Notes Accepted 1 August 2014 – 30 September 2014. Mol. Ecol. Resour. 15:228–229.

Greer KA, Hughes LM, Masternak MM. 2011. Connecting serum IGF-1, body size, and age in the domestic dog. Age (Omaha). 33:475–483.

Gunderson DR. 1997. Trade-off between reproductive effort and adult survival in oviparous and viviparous fishes. Can. J. Fish. Aquat. Sci. 54:990–998.

Hayakawa S. 2006. No cancer in cancers: Evolutionary trade-off between successful viviparity and tumor escape from the adaptive immune system. Med. Hypotheses 66:888–897.

Hiden U, Maier A, Bilban M, Ghaffari-Tabrizi N, Wadsack C, Lang I, Dohr G, Desoye G. 2006. Insulin control of placental gene expression shifts from mother to foetus over the course of pregnancy. Diabetologia 49:123–131.

Irving JA, Lala PK. 1995. Functional role of cell surface integrins on human trophoblast cell migration: Regulation by TGF-β, IGF-II, and IGFBP-1. Exp. Cell Res. 217:419–427.

Kaye MD, Jones WR, Anderson DT. 1972. Immunology and placentation in viviparous invertebrates. J. Reprod. Fertil. 31:335–336.

Kenyon CJ. 2010. The genetics of ageing. Nature 464:504–512.

Laviola L, Perrini S, Belsanti G, Natalicchio A, Montrone C, Leonardini A, Vimercati A, Scioscia M, Selvaggi L, Giorgino R, et al. 2005. Intrauterine growth restriction in humans is associated with abnormalities in placental insulin-like growth factor signaling. Endocrinology 146:1498–1505.

Leaché AD, Banbury BL, Linkem CW, De Oca ANM. 2016. Phylogenomics of a rapid radiation: Is chromosomal evolution linked to increased diversification in north american spiny lizards (Genus Sceloporus)? BMC Evol. Biol. 16:1–16.

McGaugh SE, Bronikowski AM, Kuo C-H, Reding DM, Addis EA, Flagel LE, Janzen FJ, Schwartz TS. 2015. Rapid molecular evolution across amniotes of the IIS/TOR network. Proc. Natl. Acad. Sci. 112:7055–7060.

Messier C, Teutenberg K. 2005. The Role of Insulin, Insulin Growth Factor, and Insulin-Degrading Enzyme in Brain Aging and Alzheimer' s Disease. Insulin 12:311–328.

Ostrovsky AN, Lidgard S, Gordon DP, Schwaha T, Genikhovich G, Ereskovsky A V. 2016. Matrotrophy and placentation in invertebrates: a new paradigm. Biol. Rev. 91:673–711.

Oufiero CE, Gartner GEA. 2014. The effect of parity on morphological evolution among phrynosomatid lizards. J. Evol. Biol. 27:2559–2567.

Reding DM, Addis EA, Palacios MG, Schwartz TS, Bronikowski AM. 2016. Insulin-like signaling (IIS) responses to temperature, genetic background, and growth variation in garter snakes with divergent life histories. Gen. Comp. Endocrinol. 233:88–99.

Robert KA, Thompson MB. 2000. Energy consumption by embryos of a viviparous lizard, Eulamprus tympanum, during development. Comp. Biochem. Physiol. Part A 127:481–486.

Schwartz TS, Bronikowski AM. 2011. Molecular stress pathways and the evolution of life histories in reptiles. In: Flatt T, Heyland A, editors. Mechanisms of Life History Evolution: The Genetics and Physiology of Life History Traits and Trade-Offs. OUP Oxford. p. 193–209.

Schwartz TS, Bronikowski AM. 2014. Gene expression of components of the insulin/insulin-like signaling pathway in response to heat stress in the garter snake, Thamnophis elegans. J. Iowa Acad. Sci. 121:1–4.

Sferruzzi-Perri AN, Sandovici I, Constancia M, Fowden AL. 2017. Placental phenotype and the insulin-like growth factors: resource allocation to fetal growth. J. Physiol. 595:5057–5093.

Shaffer LR, Formanowicz DR. 1996. A cost of viviparity and parental care in scorpions: reduced sprint speed and behavioural compensation. Anim. Behav. 51:1017–1024.

Shine R. 1995. A New Hypothesis for the Evolution of Viviparity in Reptiles Author. Am. Nat. 145:809–823.

Sparkman AM, Schwartz TS, Madden JA, Boyken SE, Ford NB, Serb JM, Bronikowski AM. 2012. Rates of molecular evolution vary in vertebrates for insulin-like growth factor-1

(IGF-1), a pleiotropic locus that regulates life history traits. Gen. Comp. Endocrinol. 178:164–173.

Sutter NB, Bustamante CD, Chase K, Gray MM, Zhao K, Zhu L, Padhukasahasram B, Karlins E, Davis S, Jones PG, et al. 2007. Determinant of Small Size in Dogs. Science (80-.). 247:112–115.

Talbot K, Wang H, Kazi H, Han L, Bakshi KP, Stucky A, Fuino RL, Kawaguchi KR, Samoyedny AJ, Wilson RS, et al. 2012. Demonstrated brain insulin resistance in alzheimer's disease patients is assocaited with IGF-1 resisitance, IRS-1 dysregulation, and cogntive decline. J. Clin. Invest. 122:1316–1338.

Tong M, Dong M, de la Monte SM. 2009. Brain Insulin-Like Growth Factor and Neurotrophin Resistance in Parkinson's Disease and Dementia with Lewy Bodies: Potential Role of Manganese Neurotoxicity. J. Alzheimer's Dis. 16:585–599.

Wake MH. 1993. Evolution of Oviductal Gestation in Amphibians. J. Exp. Zool. 266:394–413.

Wake MH. 2015. Fetal Adaptations for Viviparity in Amphibians. J. Morphol. 276:941–960.

Wourms JP. 1981. Viviparity: The Maternal-Fetal Relationship in Fishes. Am. Zool. 21:473–515.

Zúñiga-Vega JJ, Fuentes-G JA, Ossip-Drahos AG, Martins EP. 2016. Repeated evolution of viviparity in phrynosomatid lizards constrained interspecific diversification in some life-history traits. Biol. Lett. 12:20160653.

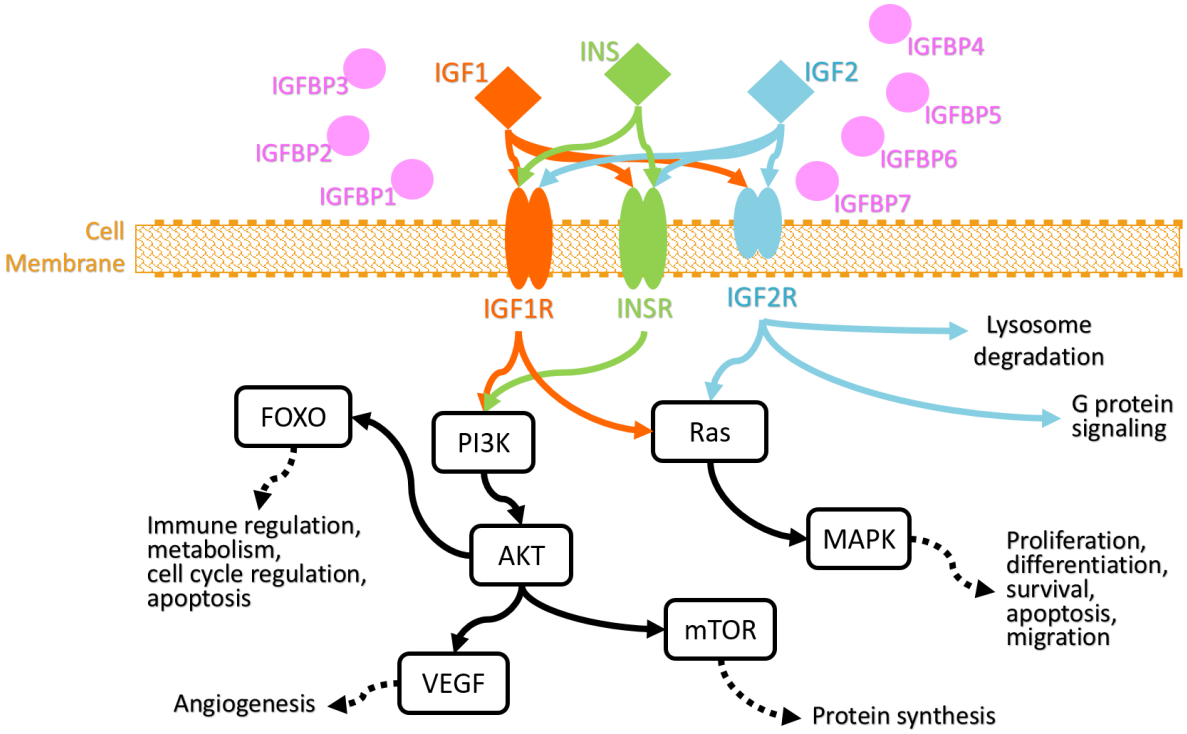

Figure 1: Simplified overview of the insulin and insulin-like signaling network and the major pathways and processes it regulates. Top regulators of the network are in purple, green orange, and blue, while the intracellular signaling cascade is in black. Abbreviations are of major genes and pathways involved such as insulin-like growth factor 1 (IGF1) and mechanistic target of rapamycin (mTOR).

Chapter 1: Identifying the relationship between evolution of the insulin and insulin-like signaling network and multiple origins of viviparity in *Sceloporus* lizards

Aundrea K. Westfall, Jamie R. Oaks & Tonia S. Schwartz

Department of Biological Sciences, Auburn University, Auburn, Alabama 36849

Keywords: *Sceloporus undulatus*, comparative genomics, Dollo's law, molecular evolution, positive selection, convergence

Introduction

The shift from egg-laying and live birth is a major life history transition seen repeatedly in vertebrate taxa. The ancestral condition of vertebrates is oviparity, where a female lays eggs within which offspring develop. However, nearly 150 vertebrate lineages have independently evolved viviparity, live birth (Blackburn 2000; Blackburn 2015a). Some authors have suggested instances in which taxa have re-evolved oviparity (Lynch and Wagner 2010; Pyron and Burbrink 2014), while others maintain that transitions back to egg laying are impossible due to Dollo's law of irreversibility: an organism never returns to a former state as it is impossible to trace back through complex phenotypes to an earlier form (Lee and Shine 1998; Blackburn 2015b). The most well-known and most extensively studied transition to viviparity occurred early in the evolution of therian mammals, the clade encompassing marsupials and placental mammals, and researchers have used robust phylogenies and ample data to clarify the history of mammalian placental evolution, diversification, and specialization (Wildman et al. 2006; Gundling and Wildman 2015; Schroeder et al. 2015; Roberts et al. 2016).

In contrast, reptiles have over 100 unique origins of viviparity. Phylogenetic analyses indicate a complex pattern of switches between oviparity and viviparity in Squamata (the order that includes lizards, snakes, and amphisbaenians), but the exact history of reproductive mode is still hotly debated among herpetologists (Pyron and Burbrink 2014; Blackburn 2015a; Blackburn 2015b). Study of viviparity in squamates has been limited to only a few clades of skinks and snakes and has primarily focused on anatomy and physiology, although some researchers have begun investigating gene expression changes during pregnancy of a few viviparous squamates (Brandley et al. 2012; Griffith et al. 2016a). In some cases, squamates have shown convergence towards the same genomic controls of placental development known in mammals, such as up-

regulation of placental lipoprotein lipase (Griffith, Ujvari, et al. 2013) and expression of Hβ58 during early placenta formation (Paulesu et al. 2001). However, squamates show a diversity in placental development, classification, and structure which exceeds that in mammals, and known cases of extra-uterine pregnancy in squamates failed to invade maternal tissues (such as in ectopic pregnancy in humans), thus indicating that squamate viviparity has evolved in fundamentally different ways from mammals (Stewart and Blackburn 1988; Griffith, Van Dyke, et al. 2013). Although there exists some evidence of convergence between mammalian and reptilian viviparity, the unique diversity and multiple origins of live birth in squamates may indicate a wide range of genetic mechanisms not yet identified.

The insulin and insulin-like signaling (IIS) network plays a vital role in a number of physiological processes, including fetal growth and development (Irving and Lala 1995; Laviola et al. 2005), aging (Kenyon 2010), life-history plasticity (Dantzer and Swanson 2012), body size (Sutter et al. 2007; Greer et al. 2011), and cognition (Messier and Teutenberg 2005; Tong et al. 2009; Talbot et al. 2012). Research has demonstrated the importance of the IIS network in mammalian viviparity, as it is crucial to the development, function, and maintenance of the placenta (Maltepe and Penn 2017; Sferruzzi-Perri et al. 2017), and dysregulation of this molecular network during fetal growth can have dramatic and often deleterious effects on the organism (Laviola et al. 2005; Forbes and Westwood 2008). Top regulators of the IIS network are insulin-like growth factors (IGF1 and IGF2), insulin (INS), their receptors (INSR, IGF1R, and IGF2R), and IGF binding proteins (IGFBP-1 through -7). These activate and interact with downstream nodes in the network to influence phosphoinositide-3 kinase (PI3K)-protein kinase B (AKT), mitogen-activated protein kinase (MAPK), mechanistic target of rapamycin (mTOR), and G-protein-coupled signaling pathways (Fig. 1.1). In mammals, both the maternal and fetal

IIS network function together to regulate many key processes, such as trophoblast proliferation, migration, and apoptosis; differentiation and vascularization of placental tissues; nutrient utilization and transport; and hormone synthesis (Hiden et al. 2006; Sferruzzi-Perri et al. 2017). In therian mammal placental development, the IIS network displays patterns of genomic imprinting in which only a single, specific parental allele for a given gene is expressed; some have proposed this epigenetic asymmetry is key to the evolution of viviparity and placentation in mammals (Moore and Haig 1991; Ferguson-Smith and Surani 2001; Reik et al. 2003; Ideraabdullah et al. 2008). However, genes identified as imprinted in mammals do not show evidence of imprinting in either live-bearing reptiles or fishes, although this work is so far limited in scope. Lawton et al. (2005) examined expression of IGF2 in two placental poeciliid fish species and found both alleles were expressed throughout development; in contrast, this gene shows variant consistent with being under significant positive selection in placental fishes while being highly conserved in mammals (O'Neill et al. 2007). In a skink with particularly advanced placentation, Griffith et al. (2016) found bi-allelic expression of 17 genes which are imprinted in mammals.

While the vast majority of IIS network research has focused on mammalian, fish, and invertebrate systems, a few researchers have recently turned their attention toward reptiles, primarily investigating evolution in the IIS related to environmental stress and life history tradeoffs (Schwartz and Bronikowski 2011; Schwartz and Bronikowski 2014; Duncan et al. 2015; Reding et al. 2016; Addis et al. 2017). In reptiles, extracellular genes in the IIS network (IGFs, their receptors, and IGFBPs) exhibit faster evolutionary rates than the rest of the genome and include many genes under positive selection, such as IGF1, IGF1R, and IGF2R (Sparkman et al. 2012; McGaugh et al. 2015). However, other genes that are under strong positive selection

in mammals are highly conserved in reptiles, such as the hormone IGF2 (McGaugh et al. 2015). Many questions about the function of this network in reptiles remain to be investigated, including details on ligand-receptor interactions, functions of top regulators IGFBPs and IGF2, and the IIS network's role in embryonic and post-natal growth (Schwartz and Bronikowski 2016). When a lineage loses the eggshell and evolves viviparity, it must evolve some form of a placenta to accommodate, at a minimum, water and gas exchange between mother and fetus. The addition of new structures and protein functions may require not only shifts in expression of genes but changes in their protein structures as well, placing selection pressure on proteins involved in exchange and transport pathways. Based on the IIS network's importance to the placenta and maternal-fetal interactions in mammals and its fundamental role in tissue proliferation, it stands to reason the IIS is likely involved in the development of placental-like structures and the repeated evolution of viviparity observed in squamates.

Lizards of the genus *Sceloporus* offer a particularly promising model to investigate origins of viviparity. They are a widespread group of approximately 100 species with a well-resolved phylogeny (Leaché et al. 2016) and have between four and six transitions to viviparity, as well as potential transitions back to oviparity. The genus has long been used as a cold-climate model of viviparity evolution, as many viviparous species occur at higher elevations. However, all viviparous species are distributed at low latitudes throughout Central America and the southern United States of America, and no extant species of *Sceloporus* has evolved viviparity in higher latitudes. These viviparous species almost all gestate during winter months, so colder winters in temperate regions may limit further range expansion of live bearing species or transitions to live-bearing in more northern species (Cruz et al. 1998). The evolution of viviparity in phrynosomatid lizards, including *Sceloporus*, has been associated with an increased rate of

evolution in morphological traits, such as in the pelvic girdle and forelimbs, and increased lineage diversification (Oufiero and Gartner 2014), but it also has been demonstrated to decrease variation in life history traits such as offspring size and relative mass, age and size at maturity, and longevity (Zúñiga-Vega et al. 2016).

We take a novel approach to understanding the evolution of viviparity in squamates by leveraging multiple independent origins in a single genus and new genomic resources to investigate the relationship between live birth and molecular evolution in a major gene network. The Genomic Resources Development Consortium et al. (2014, Appendix S2) recently published genomic resources for 35 species of *Sceloporus*, including at least one species from each potential origin of viviparity. One species, *Sceloporus occidentalis*, was sequenced using a shotgun sequencing approach, and sequencing efforts for the 34 remaining species targeted coding regions of the DNA using a reduced representation approach. However, these partial genomes have low coverage and poor quality assemblies with sparse annotation. The eastern fence lizard (*Sceloporus undulatus*) genome was recently sequenced and assembled to near chromosome-level scaffolds; it is the highest quality squamate genome to date. Here, we use the *S. undulatus* genome to improve the assemblies and annotations for the other 35 species represented from the genus, allowing us to extract IIS network genes for many of these species in this genus.

Using the genes of the IIS network, which perform major functions in the maternal-fetal interface in mammals, we can test for signatures of molecular evolution that are correlated with transitions in parity mode in *Sceloporus*, focusing on branch-site tests of positive selection and shifts in rate of evolution. If there was selection on the IIS network in the repeated evolution of viviparity, we predict to find increased rates of substitution and evidence of amino acid sites

under positive selection in multiple IIS genes at each predicted origin of viviparity. If consistent patterns of positive selection emerge for well-established transitions in parity mode, we may also be able to use these patterns to differentiate between competing hypotheses of where within the phylogeny more ambiguous transitions to viviparity occurred, as well as potential transitions back to oviparity.

Materials and Methods

Genome Assembly for Sceloporus *Species*

Raw reads from partial genome sequencing efforts of 34 *Sceloporus* species were downloaded from the Sequence Read Archive (NCBI accession numbers provided in Table 1.1). We mapped reads to the chromosomal scaffolds of the Dovetail Genomics *Sceloporus undulatus* assembly (Westfall et al., in prep) using BWA-MEM (Li 2013). The GATK 4.0 (Auwera et al. 2013; Depristo et al. 2011; McKenna et al. 2010) RealignerTargetCreator and IndelRealigner tools were used for local realignment, and HaplotypeCaller was used to identify insertion/deletion (indel) and single nucleotide polymorphism (SNP) variants between *S. undulatus* and each species using the GATK base settings. These were separated by variant type and filtered with the SelectVariants and VariantFiltration tools, also with the GATK recommended settings (SNPs: --filterExpression 'QD < 2.0 || FS > 60.0 || MQ < 40.0 || MQRankSum < -12.5 || ReadPosRankSum < -8.0'; INDELs: --filterExpression 'QD < 2.0 || FS > 200.0 || ReadPosRankSum < -20.0') . The BEDTools (Quinlan & Hall 2010) genomecov tool was used to calculate coverage and identify regions with no coverage. We generated consensus sequences for each species by writing variants back over the reference fasta, using BCFtools (Li et al. 2009) consensus for SNPs and BEDTools maskfasta for indels and regions with no mapping coverage. An ‘N’ was inserted at

each nucleotide position without coverage. Due to its exclusion from Leaché et al. (2016) because of lack of sampling, *Sceloporus utiformis* was excluded from our analyses of substitution rate and positive selection. However, because *S. utiformis* has been placed phylogenetically sister to the *S. angustus* species group in other works (Wiens and Reeder 1997; Leaché 2010), it occurs in one of the earliest diverged *Sceloporus* groups prior to the evolution of viviparity within the genus, and we feel that this does not have a significant effect on our results. All code has been made available on Github (http://github.com/akwestfall/SceloporusGenomics).

Identification and Alignment of IIS Network Gene Coding DNA Sequences

We identified 138 IIS network genes from a previous molecular evolution analysis (McGaugh et al. 2015) and reviews of the downstream IIS cascade (Pessin and Saltiel 2000; Taniguchi et al. 2006; Manning and Cantley 2007; Sferruzzi-Perri et al. 2017), focusing on the top regulators and nodes directly downstream of them (Table 1.2). Peptide sequences for each of these genes were obtained from NCBI, using either *Anolis carolinensis* (green anole, GCA_000090745.2 AnoCar2.0), *Pogona vitticeps* (bearded dragon, GCA_900067755.1 pvi1.1), *Python molurus* (Burmese python, GCA_000186305.2 Python_molurus_bivittatus-5.0.2), *Thamnophis sirtalis* (garter snake, GCA_001077635.2 Thamnophis_sirtalis-6.0), *Gallus gallus* (chick, GCA_002798355.1 Ogye1.0), or *Gekko japonicus* (Schlegel's Japanese gecko, GCA_001447785.1 Gekko_japonicus_V1.1) depending on availability, quality, and completeness of sequences (Table 1.2). These were aligned to the *S. undulatus* genome using tblastn in the BLAST+ suite (Camacho et al. 2009). Blast results were parsed by hand for multiple hits or false positive matches (e.g. paralogous genes aligning to the same region). For

each gene, we identified the region which had aligned the peptide as well as 3kb of flanking nucleotides on each end in the *S. undulatus* genome and isolated these regions from each of remaining 33 species of *Sceloporus*, and alignments across species were refined using MUSCLE (Edgar 2004). The peptides were aligned back to the region for *S. undulatus* with the Exonerate model protein2genome (Slater and Birney 2005) to generate a GFF file with predicted exon locations. Using the sequence locations identified in *S. undulatus,* exons for each gene were extracted and concatenated by position for the remaining *Sceloporus* species. For any gene in the negative direction, the reverse complement was generated with the seqtk seq -r option.

Relationship between Parity Mode Transitions and Substitution Rate Shifts

The phrynosomatid phylogeny by Leaché et al. (2016) was reduced to only include *Sceloporus* species (Fig. 1.2) and parity modes were assigned to the tips from existing literature (Sites et al. 1992; Pyron and Burbrink 2014). Ancestral states of parity mode in the genus were reconstructed using the make.simmap function in the R package 'phytools' (Revell 2012). Given a prior for parity mode transition rates, this function uses Bayesian Markov chain Monte Carlo methods to sample rates of transitions between character states and simulate the history of a character over a phylogeny (Bollback 2006). We set the ancestral state prior as oviparous and ran 1000 simulations each under two models: (1) transitions from viviparity back to oviparity are *impossible* by Dollo's law and (2) transitions from viviparity back to oviparity are *possible but unlikely* (1 in 100 transitions, on average).

To identify substitution rate differences along each branch for each IIS network gene, the phylogeny was further reduced to only 31 of the 34 species for which genomes were available (Fig. 1.3). *Sceloporus angustus*, *S. carinatus*, *S. variabilis*, and *S. smithi* were removed for

analyses due to the long branches leading to these taxa creating potentially high error rates and uncertainty in phylogenetic placement at the base of the *Sceloporus* phylogeny. In addition, these lineages have been previously identified to have lower rates of molecular evolution than the rest of the clade, as they precede the major radiation of *Sceloporus*, which could potentially bias or inflate substitution rate comparisons (Leaché et al. 2016). For each gene, we used a fixed tree topology to be consistent with the phylogeny of Leaché et al. (2016) and estimated substitution rates on each branch under a random local clock model in BEAST v1.8.4, running 10 million generations and sampling ever 1,000 generations. We used the TreeAnnotator program in BEAST to summarize rates for each branch from the posterior samples into a single tree. We compared the posterior mean rates between 7 groups of predicted viviparous branches and the background, defined as the oviparous and other viviparous branches separate from that grouping, based on stochastic character mapping results (Fig. 1.4). The mean rates of substitution were calculated for each group weighted by branch length, and the mean for the background was subtracted from each viviparous group.

To generate a null distribution for this test statistic, we performed 10,000 random permutations of parity mode transition mappings. Specifically, to generate each permutation, we drew the number of parity mode transitions according to the posterior probabilities from the stochastic character mapping analysis, and then randomly placed these transitions on the tree, enforcing the ancestral state to be oviparous. Then, for each permutation, we randomly selected a posterior sample of the rates from BEAST (without replacement) and calculated the difference in the mean rate on oviparous and viviparous branches, taking the absolute value.

These 10,000 differences in mean rates were used to estimate an empirical cumulative distribution. We found the percentiles of the true differences in mean rates between viviparous

groups and the background branches from the summary tree to calculate p-values, with significant p-values ($p \leq 0.05$, $p \leq 0.01$, $p \leq 0.005$) indicating the given group of viviparous branches are at a rate significantly different from the rest of the tree. This was repeated for every gene.

Search for Positive Selection on Branches which Transition to Viviparity

To test for positive selection among viviparous lineages in *Sceloporus*, we implemented the maximum likelihood codon substitution model (CODEML) in PAML 4.9g (Yang 2007). We used the branch-site model A, which tests for whether a defined foreground branch is more likely to contain sites with a ratio of nonsynonymous to synonymous substitution rates (ω) greater than 1 and identify sites at which significant nonsynonymous substitution is occurring (Zhang et al. 2005). This model was run for seven different foreground branches representing potential origins of viviparity (Fig. 1.4), although three branches contained only a single species sample (1 *bicanthalis*, 3 *adleri*, and 6 *clarkii*). The branch-site model is specified in the PAML control file by setting *model = 2* and *NSsites = 2*, according to the PAML 4.9 documentation. The null hypothesis is set by using *fix_omega = 1* and *omega = 1*, which fixes all ω to 1, and the alternative by setting *fix_omega = 0*, allowing variation of ω in foreground branches and therefore the possibility of positive selection. A likelihood ratio test (LRT) statistic was calculated for each tree in each gene and compared to the critical value of the χ^2 distribution with degrees of freedom $k = 1$ and significance level $\alpha = 0.05$.

Results

Genome Assemblies

A mean of 90.30% of reads for each *Sceloporus* species mapped to the *S. undulatus* reference with an average of 4.9x coverage, although this number drops to 2.0x when *S. occidentalis* is excluded (Table 1.1). The number of reads mapped for each species showed clear phylogenetic influence; the species groups closest to *S. undulatus* mapped with the highest median and smallest range (excluding outliers) compared to more diverged lineages (Fig 1.5). Of 138 IIS network genes, 117 were recovered in *S. undulatus*. Of these, 64 seem complete based on alignment with query peptides and presence of start and stop codons, while the remaining 53 are missing beginning or end regions. Each of the 117 genes have coverage from every species. The remaining 21 genes had no BLAST hits from the genome, but this does not necessarily indicate their absence in the *S. undulatus* assembly, only that the query peptides may not have been a high enough match to return results based on the tblastn algorithm.

Parity Mode Evolution in Sceloporus

Stochastic character mapping under the two different models produced fairly similar ancestral state predictions. Under the restriction of Dollo's law, simulations showed on average 5.273 transitions to viviparity (Fig. 1.6A, 1.7A). When reversals to oviparity were possible, the clade was predicted to have had averaged 5.925 transitions between states: 4.037 to viviparity and 1.88 reverse to oviparity (Fig. 1.6B, 1.7B). Both models supported a transition along the branch leading to the (*S. bicanthalis*,(*S. aeneus*, *S. subniger*)) group as well as on the branch for *S. clarkii*. The order of transitions in the clade which includes *S. formosus*, *S. adleri*, and *S. taeniocnemis* is the largest source of difference. When restricted to only forward transitions to viviparity, there are two clearly defined transitions to viviparity (asterisks on Fig. 1.6A), but when this restriction is relaxed, a single transition to viviparity occurs at an earlier branch and

the *S. cryptus/S. subpictus* lineage reverses to oviparity. The largest viviparous radiation, which includes the *S. grammicus*, *S. megalepidurus*, and *S. poinsettii* groups, experiences a single transition to viviparity in most posterior samples under Dollo's law. However, when using the model where reversals to oviparity are possible, in nearly half of the simulations, the transition is placed at an earlier bifurcation and followed by a reversal on the branch leading to *S. asper*, and in some others, the initial transition to viviparity occurs even earlier, with two reversals at *S. asper* and at *S. melanorhinus*.

Overall, seven branches with potential transitions to viviparity were identified in the reduced phylogeny of *Sceloporus* with available genomics data (Fig. 1.4), and these together created three specific groupings of viviparous species: one at *S. bicanthalis*, the transition labeled 1, hereafter referred to as *bicanthalis*; one with transitions 2-4, including the species *S. adleri*, *S. formosus*, *S. taeniocnemis*, and *S. malachiticus*, called collectively *formosus*; and one at transitions 5-7 with the species *S. clarkii*, *S. palaciosi*, *S. grammicus*, *S. torquatus*, and *S. mucronatus*, called here *grammicus*.

Shifts in Rate in Branches Transitioned to Viviparity

Of the 117 genes we evaluated for rate difference (Table 1.2), 67 had a significant rate difference associated with one or more hypothesized transitions to viviparity at an alpha level of 0.05, 30 of which were still significant at the highest significance cutoff ($p \leq 0.005$) (Table 1.3, 1.4). In the *bicanthalis* lineage, synonymous with transition 1, of the 19 genes exhibiting rate differences, only 5 remain significant at the highest cutoff: FOXO3, GNB2, IGFBP1, PIK3R6, and SHC2, although these results come from only a single species representative. In comparison, branches in the *formosus* clade experienced rate differences in 42 genes, 16 meeting the lowest p-value, and

the *grammicus* group had rate differences in 44 genes, 15 at the highest significance. Both FOXO3 and SHC2 were of highest significance in all three groups, and *formosus* and *grammicus* shared rate differences in RSP6 and SIRT4 (Table 1.5, Figure 1.8).

When looking at rate differences associated with specific transitions and not simply within clades, only a few genes showed increased rates of evolution at a single transition (Table 1.6). Two genes showed rate differences at every single tested transition, PIK3R6 and SIRT7, although these did not meet the highest alpha level, except for PIK3R6 in *bicanthalis*. Transitions 2 and 6 showed the greatest number of genes with rate differences, 36, while the fewest occurred at transition 5, where only 15 genes demonstrated a significant increase, and only one of these occurred at the highest cutoff, PTK2.

Sites under Positive Selection on Branches Leading to Viviparous Clades

Although many genes show evidence of increased rates of substitution, the null model for the branch-site test for positive selection was only rejected for 28 genes (Table 1.7). Transition 1 only showed evidence of positive selection in four genes: GNB2, PHKB, PIK3R6, and ULK3, and Transition 6 showed evidence for only two: GNB2 and GRB2. Transition 3 had no genes with evidence of positive selection. These were each of the foreground branches with only a single species, and the low numbers of genes may be attributed to lack of sampling to provide adequate power for the branch-site test. Transitions 5 and 7 showed evidence of positive selection in six and seven genes respectively, with four shared between them: PHKB, PRKAA2, RAF1, and SHC1. In addition, transition 5 rejected the null model for IGFBP1 and RASA1, and transition 7 for IGF2R, RPS6KA6, and TSC1. The highest number of genes with evidence of

selection were at transition 2, with 14 genes: FOXP1, GNB2, GRAP, IGFBP4, MKNK1, PHKB, PIK3R1, PIK3R6, PRKCG, RAF1, RICTOR, SHC3, SIRT3, and ULK2.

The only genes with positive selection shared among all three clades were PHKB and GNB2, although GNB2 only rejected the null at a single branch within the *formosus* clade, transition 3. Between the *formosus* and *grammicus* clades, RAF1 has evidence of positive selection, and between *bicanthalis* and *formosus*, only PIK3R6 showed positive selection (Figure 1.9).

In addition, a handful of genes were identified to have specific sites under positive selection. At transition 1, a single amino acid position in PHKB showed evidence of positive selection (p=0.977), and at transition 4, there were two sites in IGFBP2 (p=0.964, 0.958). Transition 2 had several genes with sites under positive selection: FOXP1 (1 site, p=0.950), IGFBP4 ((1 site, p=0.963), PIK3R6 (1 site, p=0.979), and RAF1 (1 site, p=0.960).

Discussion

We assembled genomic data for 35 species of *Sceloporus* lizards to investigate the relationship between evolution in the insulin and insulin-like signaling network and live birth. The IIS network is a major pathway in mammalian pregnancy, and it is possible it may be under pressure to evolve with the repeated evolutions of viviparity in squamate reptiles. We predicted to see a change in the difference between substitution rates of oviparous and viviparous lineages and evidence of positive selection in these genes as evidence of evolution in relation to live birth in the genus.

To understand the relationship between the IIS network evolution and parity mode, we reconstructed the history of live birth in *Sceloporus* under two models, one that did not allow

reversals from viviparity to oviparity based on Dollo's law of irreversibility and one that did allow reversals. Both models of parity mode evolution provide strong support for a single transition at the *bicanthalis* group of viviparous species. In addition, both support a single transition at the *S. clarkii* branch and then another after the bifurcation of *S. asper*. Although the alternative model allowing reversals does in some cases place earlier transitions to viviparity for that group followed by reversals at *S. melanorhinus* and *S. asper* instead, this is not the most frequently generated mapping in this group. The most significant discrepancy between both models is in the *formosus* species group, where Dollo's law supports two separate origins of viviparity and the alternative supports a single origin of viviparity followed by a reversal in the *S. cryptus/S. subpictus* lineage. Interestingly, the model that allows reversals from viviparity back to oviparity does not tend to produce the most parsimonious mapping, likely due to long-branch effects: longer branches allow more time for a transition to occur and therefore are more likely to experience a transition. For this reason, even though reversals are highly unlikely, there are two major contrasts between the models' stochastic character mappings. The branches in the *S. formosus* group where Dollo's law would place transitions are extremely short compared to the branches where the alternative model places transitions. Longer branches also contribute to the alternative model placing a forward transition to viviparity and reversal to oviparity at *S. asper* over a single forward transition after the branching of *S. asper*.

If transitions to viviparity have a relationship with evolution in the IIS network, the density of genes with significant differences in substitution rates from the background at predicted transitions may indicate greater support for the alternative model that allows for reversals. The greatest number of genes experienced increased rates of substitution at transition 2, leading to the entire *formosus* group, and when transitions 3 and 4 were considered

independently of 2, they shared increased rates in 18 of the same genes. While transitions 3 and 4 each have 33 genes with increased rates, many of these are shared with each other and transition 2, indicating that they 3 and 4 may be picking up rate differences that began at the earlier branch. In the *formosus* group, five genes, namely PHKB, IGFBP7, mTOR, JAK2, and RPS6KB1, only had significantly increased rates of substitution from transition 2, and not when 3 and 4 were considered separately. Two of these proteins have key functions in mammalian placentas. In mammals, the mTOR signaling pathway functions as a nutrient-sensing pathway and placental growth signaling sensor, integrating signals from insulin and IGFs to regulate transport molecules across the placenta. The mTOR protein forms two specific complexes, mTORC1 and mTORC2, that seem to communicate directly with placental transport systems, although the exact mechanism is still unknown (Wen et al. 2005; Shiota et al. 2006; Roos et al. 2009). IGFBP1 - IGFBP6 have long been known to be present and functioning in the mammalian placenta. However, because it is not expressed in human placentas, IGFBP7's role is only more recently being understood: it functions to promote uterine decidualization – a key process in promoting implantation and placentation in mammals (Han et al. 1996; Das 2009; Liu et al. 2012; Nawathe et al. 2016). IGFBP7 dysregulation or dysfunction has also been implicated in a number of cancers, further highlighting its importance to cell and tissue proliferation (Wajapeyee et al. 2009; Heesch et al. 2010; Vizioli et al. 2010; Chen et al. 2011; Rupp et al. 2015). That the rate of substitution in these proteins, as well as others, occurs prior to the split between two viviparous groups within *formosus* suggests that they may be under relaxed constraints and that the original transition to viviparity occurred along the branch at transition 2, and not after.

In contrast, shifts in rate in the network at the *grammicus* clade could support two separate transitions at 6 and 7, the primary prediction by both the Dollo's law and alternative

models. Transition 5 only has 15 genes with significantly increased rates (and only one at $p<0.005$), the lowest of any tested branch, while transitions 6 and 7 have 36 and 29 genes respectively. At the highest significance cutoff, these two transitions do share several genes with rate differences – namely FOXO3, GRAP, MAP3K1, PDK2, PIK3CD, RPS6, RPS6KB2, SHC2, and YWHAG – but these genes' rate differences are either not at the higher level of significance or not significant at all at transition 5. The shared rate differences between 6 and 7 but excluding 5 supports separate transitions at *S. clarkii* and then the remainder of the *grammicus* group. There may have been genomic changes occurring prior to this group's diversification which allow transition to viviparity to occur more easily. Such changes earlier in the lineage could then account for shared genes with increased rates at separate transitions if they are utilized in similar ways at the meeting of maternal and fetal tissue as a result.

Results from the CODEML branch-site test for positive selection showed a similar pattern to the substitution rate differences. In the *bicanthalis* lineage, only four genes showed evidence of positive selection. The greatest number of genes detected to be under selection were at the branch for transition 2, leading to the entire clade, with none being under selection specifically on the branch to *S. adleri*. Only four under selection at transition 4, none of which were shared with transition 2, highlighting that selection is primarily occurring throughout the entire viviparous clade beginning with the branch at transition 2. In contrast, the *grammicus* clade shows greater evidence of positive selection at transition 7 rather than earlier at transition 5, with four genes overlapping between them. Transition 6, leading to *S. clarkii*, only had two genes under positive selection. If transitions to viviparity are placing selection pressure on genes in the IIS network, our results from CODEML again support the alternative model for the *formosus* group, where there is a single transition to viviparity followed by a reversal to oviparity

at *S. cryptus/S. subpictus*. However, this hypothesis will be most strongly supported with the addition of genomic data for those oviparous species.

A few genes stand out as particularly of interest when under positive selection. Two of these are PHKB, which has evidence of positive selection in all three viviparous clades, and GNB2, which has evidence of positive selection in *S. bicanthalis*, the *formosus* group, and *S. clarkii*. Although not linked to a role specific to the placenta in mammals, PHKB is a subunit of phosphorylase kinase, and it is specifically associated with glycogenolysis, the process that breaks down glycogen in liver cells to mobilize glucose for use by cells elsewhere in the body (Hems and Whitton 1980; Terashima et al. 2014; Bhattacharya 2015). One of the major functions of the IIS network in the mammalian placenta is the transport and regulation of glucose between mother and fetus, so it stands to reason that regulation of glucose storage and mobilization may be affected by transitions to viviparity. G protein subunit beta 2 (GNB2) is a guanine nucleotide binding protein subunit that has a role in a wide range of intracellular signaling pathways, primarily by regulating concentrations of secondary messengers such as cAMP, diacylglycerol, and sodium and calcium cations (Svoboda et al. 2004). Another gene under selection in more than one clade is RAF1 in both the *formosus* and *grammicus* groups. This is a major regulatory component of the MAPK pathway that regulates cell cycle progression and cell proliferation; defects in this network are associated with uncontrolled growth in many cancers. However, RAF1 is not typically implicated in human carcinogenesis, but rather a paralog, BRAF (Emuss et al. 2005). RAF1's regulatory function in cell proliferation may be under selection to promote cell proliferation at the meeting of maternal-fetal tissue to form early placenta-like structures. Of the two genes which share increased substitution rates across all three viviparous groups, one additionally shows evidence of positive selection in both the *bicanthalis* and *formosus* groups:

PIK3R6. This protein forms a heterodimer with PIK3CG, where it functions as a regulatory subunit and PIK3CG as a catalytic subunit. As a heterodimer, it is a major stimulator of angiogenesis in the PI3K pathway (Wilson et al. 2011; Liu et al. 2018).

Although they show evidence of evolution in other clades, IGF1 and IGF2, major signaling molecules for the IIS network, exhibit neither increased rates of substitution or positive selection associated with live birth in this group. These genes may exhibit higher conservation within the genus to preserve their functional role in other organs and processes in the body. However, their receptors and molecules which complex with the receptors do. Insulin receptor substrate 1 (IRS1), insulin receptor substrate 4 (IRS4), and IGF1R all show increased rates of substitution within the *formosus* group and in *S. clarkii*, and IGF2R is under positive selection at transition 7 (the *grammicus* group excluding *S. clarkii*). Many of the IGF binding proteins show increased rate shifts at all transitions, primarily IGFBP1, IGFBP2, IGFBP4, and IGFBP7, and each of these is also under positive selection in one predicted transition to viviparity. The IGFBPs are responsible for regulation of IGF availability to the receptors, and they are expressed in a variety of tissues throughout development. In mammals, they are all expressed in various species' placentas. Their evolution in this clade relative to viviparous species may indicate that they are adapting to new regulatory roles in the structure and function of placenta-like structures that form at the maternal-fetal interface following the loss of the eggshell.

The results presented here do suggest there is an evolutionary relationship between live birth and the insulin and insulin-like signaling network in *Sceloporus* lizards. However, more work is needed to better clarify the role of the IIS network in these viviparous species. Sequences at regulatory regions for these genes could provide molecular evidence for changes in regulation for these genes across different clades. A few key species' genomes, including *S. cryptus*, *S.*

subpictus, *S. melanorhinus*, and more viviparous species would improve sampling for detection of rate shifts and positive selection, and it would also allow better distinction of how the network is evolving at putative transitions to viviparity, including to support whether or not a reversal to oviparity occurred in this group at the branch to *S. cryptus/S. subpictus.* In addition, transcriptomic and proteomic from reproductive uterus and fetal membranes from both oviparous and viviparous species would provide insight to how the network is being expressed and activated differently between the two states and across different origins of viviparity.

References

Addis EA, Gangloff EJ, Palacios MG, Carr KE, Bronikowski AM. 2017. Merging the "morphology-performance-fitness" paradigm and life-history theory in the eagle lake garter snake research project. Integr. Comp. Biol. 57:423–435.

Auwera GA Van Der, Carneiro MO, Hartl C, Poplin R, Levy-moonshine A, Jordan T, Shakir K, Roazen D, Thibault J, Banks E, et al. 2013. From FastQ data to high confidence varant calls: the Genonme Analysis Toolkit best practices pipeline. Curr. Protoc. Bioinforma. 43:11.10.1-11.10.33.

Bhattacharya K. 2015. Investigation and management of the hepatic glycogen storage diseases. Transl. Pediatr. 4:240–248.

Blackburn DG. 2000. Classification of the Reproductive Patterns of Amniotes. Herpetol. Monogr. 14:371–377.

Blackburn DG. 2015a. Evolution of vertebrate viviparity and specializations for fetal nutrition: A quantitative and qualitative analysis. J. Morphol. 276:961–990.

Blackburn DG. 2015b. Evolution of viviparity in squamate reptiles: Reversibility reconsidered. J. Exp. Zool. Part B Mol. Dev. Evol. 324:473–486.

Bollback JP. 2006. SIMMAP: Stochastic character mapping of discrete traits on phylogenies. BMC Bioinformatics 7:1–7.

Brandley MC, Young RL, Warren DL, Thompson MB, Wagner GP. 2012. Uterine gene expression in the live-bearing lizard, Chalcides ocellatus, reveals convergence of squamate reptile and mammalian pregnancy mechanisms. Genome Biol. Evol. 4:394–411.

Camacho C, Coulouris G, Avagyan V, Ma N, Papadopoulos J, Bealer K, Madden TL. 2009. BLAST+: Architecture and applications. BMC Bioinformatics 10:1–9.

Chen D, Yoo BK, Santhekadur PK, Gredler R, Bhutia SK, Das SK, Fuller C, Su Z -z., Fisher PB, Sarkar D. 2011. Insulin-like Growth Factor-Binding Protein-7 Functions as a Potential Tumor Suppressor in Hepatocellular Carcinoma. Clin. Cancer Res. 17:6693–6701.

Cruz FR. M la, Cruz MV-S, Andrews RM. 1998. Evolution of Viviparity in the Lizard Genus Sceloporus. Herpetologica 54:521–532.

Dantzer B, Swanson EM. 2012. Mediation of vertebrate life histories via insulin-like growth factor-1. Biol. Rev. 87:414–429.

Das SK. 2009. Cell cycle regulatory control for uterine stromal cell decidualization in implantation. Reproduction 137:889–899.

Depristo MA, Banks E, Poplin R, Garimella K V., Maguire JR, Hartl C, Philippakis AA, Del Angel G, Rivas MA, Hanna M, et al. 2011. A framework for variation discovery and genotyping using next-generation DNA sequencing data. Nat. Genet. 43:491–501.

Duncan CA, Jetzt AE, Cohick WS, John-Alder HB. 2015. Nutritional modulation of IGF-1 in relation to growth and body condition in Sceloporus lizards. Gen. Comp. Endocrinol. 216:116–124.

Edgar RC. 2004. MUSCLE: Multiple sequence alignment with high accuracy and high throughput. Nucleic Acids Res. 32:1792–1797.

Emuss V, Garnett M, Mason C, Marais R. 2005. Mutations of C-RAF are rare in human cancer because C-RAF has a low basal kinase activity compared with B-RAF. Cancer Res. 65:9719–9726.

Ferguson-Smith AC, Surani MA. 2001. Imprinting and the epigenetic asymmetry between parental genomes. Science (80-.). 293:1086–1089.

Forbes K, Westwood M. 2008. The IGF axis and placental function: A mini review. Horm. Res. 69:129–137.

Genomic Resources Development Consortium, Arthofer W, Banbury BL, Carneiro M, Cicconardi F, Duda TF, Nolte V, Nourisson C, Harris RB, Kang DS, et al. 2014. Genomic Resources Notes Accepted 1 August 2014 – 30 September 2014. Mol. Ecol. Resour. 15:228–229.

Greer KA, Hughes LM, Masternak MM. 2011. Connecting serum IGF-1, body size, and age in the domestic dog. Age (Omaha). 33:475–483.

Griffith OW, Brandley MC, Belov K, Thompson MB. 2016a. Reptile pregnancy is underpinned by complex changes in uterine gene expression: A comparative analysis of the uterine transcriptome in viviparous and oviparous lizards. Genome Biol. Evol. 8:3226–3239.

Griffith OW, Brandley MC, Belov K, Thompson MB. 2016b. Allelic expression of mammalian imprinted genes in a matrotrophic lizard, Pseudemoia entrecasteauxii. Dev. Genes Evol. 226:79–85.

Griffith OW, Van Dyke JU, Thompson MB. 2013. No implantation in an extra-uterine pregnancy of a placentotrophic reptile. Placenta 34:510–511.

Griffith OW, Ujvari B, Belov K, Thompson MB. 2013. Placental lipoprotein lipase (LPL) gene expression in a placentotrophic lizard, Pseudemoia entrecasteauxii. J. Exp. Zool. Part B Mol. Dev. Evol. 320:465–470.

Gundling WE, Wildman DE. 2015. A review of inter- and intraspecific variation in the eutherian placenta. Philos. Trans. R. Soc. B Biol. Sci. 370:20140072–20140072.

Han VKM, Bassett N, Walton J, Challis JRG. 1996. The Expression of Insulin-Like Growth Factor (IGF) and IGF-Binding Protein (IGFBP) genes in the Human Placenta and

Membranes: Evidence for IGF-IGFBP Interactions at the Feto-Maternal Interface. J. Clin. Endocrinol. Metab. 81:2680–2693.

Heesch S, Schlee C, Neumann M, Stroux A, Kühnl A, Schwartz S, Haferlach T, Goekbuget N, Hoelzer D, Thiel E, et al. 2010. BAALC-associated gene expression profiles define IGFBP7 as a novel molecular marker in acute leukemia. Leukemia 24:1429–1436.

Hems DA, Whitton PD. 1980. Control of Hepatic Glycogenolysis. Physiol. Rev. 60:1–50.

Hiden U, Maier A, Bilban M, Ghaffari-Tabrizi N, Wadsack C, Lang I, Dohr G, Desoye G. 2006. Insulin control of placental gene expression shifts from mother to foetus over the course of pregnancy. Diabetologia 49:123–131.

Ideraabdullah FY, Vigneau S, Bartolomei MS. 2008. Genomic imprinting mechanisms in mammals. Mutat. Res. Mol. Mech. Mutagen. 647:77–85.

Irving JA, Lala PK. 1995. Functional role of cell surface integrins on human trophoblast cell migration: Regulation by TGF-β, IGF-II, and IGFBP-1. Exp. Cell Res. 217:419–427.

Kenyon CJ. 2010. The genetics of ageing. Nature 464:504–512.

Laviola L, Perrini S, Belsanti G, Natalicchio A, Montrone C, Leonardini A, Vimercati A, Scioscia M, Selvaggi L, Giorgino R, et al. 2005. Intrauterine growth restriction in humans is associated with abnormalities in placental insulin-like growth factor signaling. Endocrinology 146:1498–1505.

Lawton BR, Sevigny L, Obergfell C, Reznick D, O'Neill RJ, O'Neill MJ. 2005. Allelic expression of IGF2 in live-bearing, matrotrophic fishes. Dev. Genes Evol. 215:207–212.

Leaché AD. 2010. Species trees for spiny lizards (Genus Sceloporus): Identifying points of concordance and conflict between nuclear and mitochondrial data. Mol. Phylogenet. Evol. 54:162–171.

Leaché AD, Banbury BL, Linkem CW, De Oca ANM. 2016. Phylogenomics of a rapid radiation: Is chromosomal evolution linked to increased diversification in north american spiny lizards (Genus Sceloporus)? BMC Evol. Biol. 16:1–16.

Lee MSY, Shine R. 1998. Reptilian Viviparity and Dollo's Law. Evolution (N. Y). 52:1441–1450.

Li H. 2013. Aligning sequence reads, clone sequences and assembly contigs with BWA-MEM. 0:1–3. Available from: http://arxiv.org/abs/1303.3997

Li H, Handsaker B, Wysoker A, Fennell T, Ruan J, Homer N, Marth G, Abecasis G, Durbin R. 2009. The Sequence Alignment/Map format and SAMtools. Bioinformatics 25:2078–2079.

Liu X, Xu Y, Zhou Q, Chen M, Zhang Y, Liang H, Zhao J, Zhong W, Wang M. 2018. PI3K in cancer: Its structure, activation modes and role in shaping tumor microenvironment. Futur. Oncol. 14:665–674.

Liu ZK, Wang RC, Han BC, Yang Y, Peng JP. 2012. A Novel Role of IGFBP7 in Mouse Uterus: Regulating Uterine Receptivity through Th1/Th2 Lymphocyte Balance and Decidualization. PLoS One 7:3–10.

Lynch VJ, Wagner GP. 2010. Did egg-laying boas break dollo's law? Phylogenetic evidence for reversal to oviparity in sand boas (Eryx: Boidae). Evolution (N. Y). 64:207–216.

Maltepe E, Penn AA. 2017. Development, Function, and Pathology of the Placenta. In: Gleason CA, editor. Avery's Diseases of the Newborn. 10th ed. p. 40–60.e8.

Manning BD, Cantley LC. 2007. AKT/PKB Signaling: Navigating Downstream. Cell 129:1261–1274.

McGaugh SE, Bronikowski AM, Kuo C-H, Reding DM, Addis EA, Flagel LE, Janzen FJ, Schwartz TS. 2015. Rapid molecular evolution across amniotes of the IIS/TOR network. Proc. Natl. Acad. Sci. 112:7055–7060.

McKenna A, Hanna M, Banks E, Sivachenko A, Cibulskis K, Kernytsky A, Garimella K, Altschuler D, Gabriel S, Daly M, et al. 2010. The Genome Analysis Toolkit: a MapReduce framework for analyzing next-generation DNA sequencing. Genome Res. 20:1297–1303.

Messier C, Teutenberg K. 2005. The Role of Insulin, Insulin Growth Factor, and Insulin-Degrading Enzyme in Brain Aging and Alzheimer' s Disease. Insulin 12:311–328.

Moore TOM, Haig D. 1991. Genomic imprinting in mammalian development: a parental tug-of-war. Trends Genet. 7:45–49.

Nawathe AR, Christian M, Kim SH, Johnson M, Savvidou MD, Terzidou V. 2016. Insulin-like growth factor axis in pregnancies affected by fetal growth disorders. Clin. Epigenetics 8:1–13.

O'Neill MJ, Lawton BR, Mateos M, Carone DM, Ferreri GC, Hrbek T, Meredith RW, Reznick DN, O'Neill RJ. 2007. Ancient and continuing Darwinian selection on insulin-like growth factor II in placental fishes. Proc. Natl. Acad. Sci. U. S. A. 104:12404–12409.

Oufiero CE, Gartner GEA. 2014. The effect of parity on morphological evolution among phrynosomatid lizards. J. Evol. Biol. 27:2559–2567.

Paulesu L, Cateni C, Romagnoli R, Chellini F, Angelini F, Guarino FM, Rider V, Imakawa K, Bigliardi E. 2001. Evidence of Hβ58, a gene involved in mammalian placental development, in the three-toed skink, Chalcides chalcides (Squamata: Scincidae), a viviparous placentotrophic reptile. Placenta 22:735–741.

Pessin JE, Saltiel AR. 2000. Signaling pathways in insulin action: molecular targets of insulin resistance. J. Clin. Invest. 106:165–170.

Pyron RA, Burbrink FT. 2014. Early origin of viviparity and multiple reversions to oviparity in squamate reptiles. Ecol. Lett. 17:13–21.

Quinlan AR, Hall IM. 2010. BEDTools: A flexible suite of utilities for comparing genomic features. Bioinformatics 26:841–842.

Reding DM, Addis EA, Palacios MG, Schwartz TS, Bronikowski AM. 2016. Insulin-like signaling (IIS) responses to temperature, genetic background, and growth variation in garter snakes with divergent life histories. Gen. Comp. Endocrinol. 233:88–99.

Reik W, Constância M, Fowden A, Anderson N, Dean W, Ferguson-Smith A, Tycko B, Sibley C. 2003. Regulation of supply and demand for maternal nutrients in mammals by imprinted genes. J. Physiol. 547:35–44.

Revell LJ. 2012. phytools: An R package for phylogenetic comparative biology (and other things). Methods Ecol. Evol. 3:217–223.

Roberts RM, Green JA, Schulz LC. 2016. The evolution of the placenta. Reproduction 152:R179–R189.

Roos S, Powell TL, Jansson T. 2009. Placental mTOR links maternal nutrient availability to fetal growth. Biochem. Soc. Trans. 37:295–298.

Rupp C, Scherzer M, Rudisch A, Unger C, Haslinger C, Schweifer N, Artaker M, Nivarthi H, Moriggl R, Hengstschläger M, et al. 2015. IGFBP7, a novel tumor stroma marker, with growth-promoting effects in colon cancer through a paracrine tumor-stroma interaction. Oncogene 34:815–825.

Schroeder DI, Jayashankar K, Douglas KC, Thirkill TL, York D, Dickinson PJ, Williams LE, Samollow PB, Ross PJ, Bannasch DL, et al. 2015. Early Developmental and Evolutionary Origins of Gene Body DNA Methylation Patterns in Mammalian Placentas. PLoS Genet. 11:1–20.

Schwartz TS, Bronikowski AM. 2011. Molecular stress pathways and the evolution of life histories in reptiles. In: Flatt T, Heyland A, editors. Mechanisms of Life History Evolution: The Genetics and Physiology of Life History Traits and Trade-Offs. OUP Oxford. p. 193–209.

Schwartz TS, Bronikowski AM. 2014. Gene expression of components of the insulin/insulin-like signaling pathway in response to heat stress in the garter snake, Thamnophis elegans. J. Iowa Acad. Sci. 121:1–4.

Schwartz TS, Bronikowski AM. 2016. Evolution and Function of the Insulin and Insulin-like Signaling Network in Ectothermic Reptiles: Some Answers and More Questions. Integr. Comp. Biol. 56:171–184.

Sferruzzi-Perri AN, Sandovici I, Constancia M, Fowden AL. 2017. Placental phenotype and the insulin-like growth factors: resource allocation to fetal growth. J. Physiol. 595:5057–5093.

Shiota C, Woo JT, Lindner J, Shelton KD, Magnuson MA. 2006. Multiallelic Disruption of the rictor Gene in Mice Reveals that mTOR Complex 2 Is Essential for Fetal Growth and Viability. Dev. Cell 11:583–589.

Sites JW, Archie JW, Cole CJ, Villela OF. 1992. A Review of Phylogenetic Hypotheses for Lizards of the Genus Sceloporus (Phrynosomatidae) - Implications for Ecological and Evolutionary Studies. Bull. Am. Museum Nat. Hist.:1–110.

Slater GSC, Birney E. 2005. Automated generation of heuristics for biological sequence comparison. BMC Bioinformatics 6:1–11.

Sparkman AM, Schwartz TS, Madden JA, Boyken SE, Ford NB, Serb JM, Bronikowski AM. 2012. Rates of molecular evolution vary in vertebrates for insulin-like growth factor-1 (IGF-1), a pleiotropic locus that regulates life history traits. Gen. Comp. Endocrinol. 178:164–173.

Stewart JR, Blackburn DG. 1988. Reptilian Placentation: Structural Diversity and Terminology. Copeia 1988:839–852.

Sutter NB, Bustamante CD, Chase K, Gray MM, Zhao K, Zhu L, Padhukasahasram B, Karlins E, Davis S, Jones PG, et al. 2007. Determinant of Small Size in Dogs. Science (80-.). 247:112–115.

Svoboda P, Teisinger J, Novotný J, Bouřová L, Drmota T, Hejnová L, Moravcová Z, Lisý V, Rudajev V, Stöhr J, et al. 2004. Biochemistry of Transmembrane Signaling Mediated by Trimeric G Proteins. Physiol. Res. 53:S141–S152.

Talbot K, Wang H, Kazi H, Han L, Bakshi KP, Stucky A, Fuino RL, Kawaguchi KR, Samoyedny AJ, Wilson RS, et al. 2012. Demonstrated brain insulin resistance in alzheimer's disease patients is assocaited with IGF-1 resisitance, IRS-1 dysregulation, and cogntive decline. J. Clin. Invest. 122:1316–1338.

Taniguchi CM, Emanuelli B, Kahn CR. 2006. Critical nodes in signalling pathways: insights into insulin action. Nat. Rev. Mol. Cell Biol. 7:85–96.

Terashima M, Fujita Y, Togashi Y, Sakai K, De Velasco M a, Tomida S, Nishio K. 2014. KIAA1199 interacts with glycogen phosphorylase kinase β-subunit (PHKB) to promote glycogen breakdown and cancer cell survival. Oncotarget 5:7040–7050.

Tong M, Dong M, de la Monte SM. 2009. Brain Insulin-Like Growth Factor and Neurotrophin Resistance in Parkinson's Disease and Dementia with Lewy Bodies: Potential Role of Manganese Neurotoxicity. J. Alzheimer's Dis. 16:585–599.

Vizioli MG, Sensi M, Miranda C, Cleris L, Formelli F, Anania MC, Pierotti MA, Greco A. 2010. IGFBP7: An oncosuppressor gene in thyroid carcinogenesis. Oncogene 29:3835–3844.

Wajapeyee N, Kapoor V, Mahalingam M, Green MR. 2009. Efficacy of IGFBP7 for treatment of metastatic melanoma and other cancers in mouse models and human cell lines. Mol. Cancer Ther. 8:3009–3014.

Wen HY, Abbasi S, Kellems RE, Xia Y. 2005. mTOR: A placental growth signaling sensor. Placenta 26.

Wiens JJ, Reeder TW. 1997. Phylogeny of the Spiny Lizards (Sceloporus) Based on Molecular and Morphological Evidence. Herpetol. Monogr. 11:1–101.

Wildman DE, Chen C, Erez O, Grossman LI, Goodman M, Romero R. 2006. Evolution of the mammalian placenta revealed by phylogenetic analysis. Proc. Natl. Acad. Sci. U. S. A. 103:3203–3208.

Wilson LS, Baillie GS, Pritchard LM, Umana B, Terrin A, Zaccolo M, Houslay MD, Maurice DH. 2011. A phosphodiesterase 3B-based signaling complex integrates exchange protein activated by cAMP 1 and phosphatidylinositol 3-kinase signals in human arterial endothelial cells. J. Biol. Chem. 286:16285–16296.

Yang Z. 2007. PAML 4: Phylogenetic analysis by maximum likelihood. Mol. Biol. Evol. 24:1586–1591.

Zhang J, Nielsen R, Yang Z. 2005. Evaluation of an improved branch-site likelihood method for detecting positive selection at the molecular level. Mol. Biol. Evol. 22:2472–2479.

Zúñiga-Vega JJ, Fuentes-G JA, Ossip-Drahos AG, Martins EP. 2016. Repeated evolution of viviparity in phrynosomatid lizards constrained interspecific diversification in some life-history traits. Biol. Lett. 12:20160653.

Table 1.1: NCBI SRA accession numbers of raw data for *Sceloporus* species used. For boxes with "NA**" a number was not reported in the original publication.

Species Epithet	SRA Accession	No. of Raw Reads	No. Reads in Original Assembly	No. Reads Mapped	Avg. Coverage	St. Dev. Coverage
adleri	SRS606714	61,396,744	31,351,090	57623356	2.57	11.29
angustus	SRS606715	59,008,874	28,606,707	53240570	1.55	8.25
bicanthalis	SRS606716	50,963,292	31,215,601	47490393	1.95	11.25
carinatus	SRS606717	79,553,536	46,700,905	71614592	1.93	10.31
clarkii	SRS606743	NA**	18,542,404	37267500	1.41	10.45
cowlesi	SRS606718	48,762,864	26,224,281	46941389	2.27	7.34
edwardtaylori	SRS606719	45,692,228	23,424,584	44937557	2.05	14.74
exsul	SRS606720	35,733,442	14,996,169	33706829	1.25	8.76
formosus	SRS606721	64,971,516	35,813,869	63964457	2.95	10.76
gadoviae	SRS606722	58,190,400	26,021,380	53013235	1.97	12.82
graciosus	SRS606746	NA**	10,215,985	42752450	1.57	12.66
grammicus	SRS606723	47,583,134	25,273,167	46957278	2.01	9.91
horridus	SRS606724	37,356,428	19,275,595	35566121	1.60	7.40
hunsakeri	SRS606725	44,180,416	25,580,920	41803427	1.51	9.34
jalapae	SRS606726	69,585,852	38,721,933	64221394	2.41	10.03
licki	SRS606727	33,801,198	16,485,334	31567146	1.32	8.75
magister	SRS606728	34,953,494	17,964,775	31906981	1.14	7.48
malachiticus	SRS606747	NA**	21,965,000	45029168	1.80	10.87
mucronatus	SRS606729	55,355,942	26,574,363	52396924	2.26	11.46
occidentalis	SRS609406	NA**	40,849,442	369535375	17.39	29.99
ochoterenae	SRS606730	66,333,598	31,248,947	56394745	1.89	12.37
olivaceus	SRS606731	31,389,948	16,658,706	29033817	1.34	6.12
orcutti	SRS606732	38,845,798	23,213,887	36467744	1.32	9.59
palaciosi	SRS606733	65,853,622	32,395,045	58317757	2.39	14.07
scalaris	SRS606734	33,561,800	24,697,422	58293959	2.38	12.63
smithi	SRS606736	47,525,652	25,097,617	47151159	1.43	11.65
spinosus	SRS606737	59,078,332	32,562,785	58294846	2.72	8.92
taeniocnemis	SRS606745	NA**	17,959,114	34684020	1.37	7.44
torquatus	SRS606738	67,811,820	33,838,916	60680088	2.47	14.13
tristichus	SRS606739	53,101,800	31,013,091	50840689	2.46	7.91
utiformis	SRS606744	NA**	15,587,168	38036779	0.84	5.78
variabilis	SRS606740	75,896,002	44,504,186	74442237	2.21	14.40
woodi	SRS606741	35,209,562	15,225,180	33290873	1.55	5.44
zosteromus	SRS606742	23,051,026	9,746,243	21565437	0.90	4.81

Table 1.2: NCBI accession numbers and species of each gene used in BLAST to identify IIS genes. Genes which were found in *S. undulatus* are indicated by a Y in the rightmost column.

Gene ID	Gene Name	Species Reference	NCBI Accession	Found?
AKT1S1	Proline-rich AKT substrate 1	*Anolis carolinensis*	XP_003230365.1	Y
CAB39L	Calcium-binding protein 39-like	*Gekko japonicus*	XP_015270199.1	N
CALM1	Calmodulin 1	*Anolis carolinensis*	XP_008112670.1	Y
CCND1	Cyclin D1	*Anolis carolinensis*	XP_003214708.2	Y
EIF4E	Eukaryotic translation factor 4E	*Anolis carolinensis*	XP_003225575.1	Y
EIF4E2	Eukaryotic translation factor 4E type 2	*Anolis carolinensis*	XP_008116054.1	Y
ELK1	ETS domaining-containing protein	*Anolis carolinensis*	XP_003216750.2	Y
FOS	Proto-oncogene c-Fos	*Pogona vitticeps*	XP_020649581.1	Y
FOXA1	Hepatocyte nuclear factor 3-alpha	*Anolis carolinensis*	XP_008101045.1	Y
FOXA2	Hepatocyte nuclear factor 3-beta	*Thamnophis sirtalis*	XP_013926879.1	N
FOXF1	Forkhead box protein F1	*Pogona vitticeps*	XP_020664127.1	Y
FOXJ1	Forkhead box protein J1	*Anolis carolinensis*	XP_003217292.1	Y
FOXJ2	Forkhead box protein J2	*Anolis carolinensis*	XP_008114117.1	Y
FOXK1	Forkhead box protein K1	*Anolis carolinensis*	XP_008119932.2	Y
FOXK2	Forkhead box protein K2	*Anolis carolinensis*	XP_003217197.2	N
FOXN2	Forkhead box protein N2	*Anolis carolinensis*	XP_016846200.1	Y
FOXN3	Forkhead box protein N3	*Anolis carolinensis*	XP_008113670.1	Y
FOXO1	Forkhead box protein O1	*Anolis carolinensis*	XP_003215340.1	Y
FOXO3	Forkhead box protein O3	*Pogona vitticeps*	XP_020656989.1	Y
FOXO4	Forkhead box protein O4	*Pogona vitticeps*	XP_020651543.1	Y
FOXP1	Forkhead box protein P1	*Anolis carolinensis*	XP_008103588.1	Y
FOXP4	Forkhead box protein P4	*Anolis carolinensis*	XP_008107899.1	Y
GNA11	G protein subunit α11	*Anolis carolinensis*	XP_003228816.2	N
GNAI3	G protein subunit αI3	*Anolis carolinensis*	XP_003220230.1	Y
GNB2	G protein subunuit β2	*Anolis carolinensis*	XP_008122386.1	Y
GNB5	G protein subunuit β5	*Anolis carolinensis*	XP_008118742.1	Y
GRAP	GRB2-related adaptor protein	*Anolis carolinensis*	XP_003228353.1	Y
GRB2	Growth factor receptor bound protein 2	*Anolis carolinensis*	XP_003217257.1	Y
GSK3A	Glycogen synthase kinase 3α	*Anolis carolinensis*	NP_001268643.1	Y
GSK3B	Glycogen synthase kinase 3β	*Anolis carolinensis*	XP_003226832.1	N

HRAS	GTPase HRas	*Anolis carolinensis*	XP_016849026.1	N
IGF1	Insulin-like growth factor 1	*Anolis carolinensis*	XP_008108777.1	Y
IGF1R	Insulin-like growth factor 1 receptor	*Anolis carolinensis*	XP_003226539.2	Y
IGF2	Insulin-like growth factor 2	*Anolis carolinensis*	XP_008106134.1	Y
IGF2R	Cation-independent mannose-6-phosphate receptor	*Anolis carolinensis*	XP_008121462.1	Y
IGFBP1	IGF binding protein 1	*Anolis carolinensis*	XP_003222343.1	Y
IGFBP2	IGF binding protein 2	*Anolis carolinensis*	XP_016853564.1	Y
IGFBP3	IGF binding protein 3			
IGFBP4	IGF binding protein 4	*Pogona vitticeps*	XP_020661537.1	Y
IGFBP5	IGF binding protein 5	*Anolis carolinensis*	XP_003215002.2	Y
IGFBP7	IGF binding protein 7	*Anolis carolinensis*	XP_008114855.1	Y
IKBKB	Inhibitor of nuclear factor kappa-B kinase subunit β	*Anolis carolinensis*	XP_016853156.1	Y
INPP5A	Inositol polyphosphate-5-phosphatase A	*Anolis carolinensis*	XP_008104921.1	Y
INPPL1	Insositol polyphosphatase like 1	*Anolis carolinensis*	XP_008122032.1	Y
INS	Insulin	*Anolis carolinensis*	XP_003214805.1	N
INSR	Insulin receptor	*Anolis carolinensis*	XP_003230413.2	Y
IRS1	Insulin receptor substrate 1	*Anolis carolinensis*	XP_003218341.1	Y
IRS2	Insulin receptor substrate 2	*Pogona vitticeps*	XP_020670494.1	Y
IRS4	Insulin receptor substrate 4	*Thamnophis sirtalis*	XP_013921369.1	Y
JAK1	Janus kinase 1	*Anolis carolinensis*	XP_008107519.1	Y
JAK2	Janus kinase 2	*Anolis carolinensis*	XP_003216540.1	Y
KL	Klotho precursor	*Anolis carolinensis*	XP_008122056.1	Y
KRAS	Kirsten ras oncogene	*Gallus gallus*	NP_001243091.1	Y
MAP2K1	Mitogen-activated protein kinase kinase 1	*Pogona vitticeps*	XP_020661331.1	N
MAP2K2	Mitogen-activated protein kinase kinase 2	*Python molurus*	XP_007434444.2	Y
MAP2K3	Mitogen-activated protein kinase kinase 3	*Anolis carolinensis*	XP_003226578.3	Y
MAP2K4	Mitogen-activated protein kinase kinase 4	*Anolis carolinensis*	XP_008102522.1	Y
MAP3K1	Mitogen-activated protein kinase kinase kinase 1	*Anolis carolinensis*	XP_016846352.1	Y

MAP3K10	Mitogen-activated protein kinase kinase kinase 10	*Anolis carolinensis*	XP_003222932.2	Y
MAPK10	Mitogen-activated protein kinase 10	*Pogona vitticeps*	XP_020661048.1	N
MAPK3	Mitogen-activated protein kinase 3	*Anolis carolinensis*	XP_016851543.1	Y
MDM2	Mouse double minute 2	*Anolis carolinensis*	XP_008114806.2	Y
MDM4	Mouse double minute 4	*Anolis carolinensis*	XP_003220455.1	Y
MKNK1	MAP kinase-interacting serine/threonine-protein kinase 1	*Anolis carolinensis*	XP_008107761.1	Y
MLST8	Target of rapamycin complex subunit LST8	*Anolis carolinensis*	XP_008121323.1	Y
MRAS	Muscle RAS oncogene	*Anolis carolinensis*	XP_003214967.1	Y
MTOR	Mechanistic target of rapamycin	*Anolis carolinensis*	XP_008120094.2	Y
NRAS	Neuroblastoma RAS viral oncogene	*Anolis carolinensis*	XP_003220530.1	Y
NRF1	Nuclear respiratory factor 1	*Anolis carolinensis*	XP_008120380.1	Y
PDE3B	cGMP-inhibited 3',5'-cyclic phosphodiesterase B	*Anolis carolinensis*	XP_008105416.1	Y
PDK1	Pyruvate dehydrogenase kinase 1	*Anolis carolinensis*	XP_003226208.1	Y
PDK2	Pyruvate dehydrogenase kinase 2	*Anolis carolinensis*	XP_008111728.1	Y
PDK3	Pyruvate dehydrogenase kinase 3	*Anolis carolinensis*	XP_003218894.1	Y
PDPK1	Phosphoinositide-dependent kinase-1	*Anolis carolinensis*	XP_003228307.1	Y
PHKB	Phosphorylase kinase β-subunit	*Pogona vitticeps*	XP_020643941.1	Y
PHKG1	Phosphorylase kinase catalytic subunit gamma 1	*Pogona vitticeps*	XP_020659556.1	Y
PIK3CA	Phosphoinositide-3-kinase, catalytic, α polypeptide	*Anolis carolinensis*	XP_003218156.1	Y
PIK3CB	Phosphoinositide-3-kinase, catalytic, β polypeptide	*Anolis carolinensis*	XP_003218352.1	Y
PIK3CD	Phosphoinositide-3-kinase, catalytic, δ polypeptide	*Anolis carolinensis*	XP_008111838.1	Y

PIK3CG	Phosphoinositide-3-kinase, catalytic, γ polypeptide	*Anolis carolinensis*	XP_008109773.1	Y
PIK3R1	Phosphatidylinositol 3-kinase regulatory subunit α	*Anolis carolinensis*	XP_003216391.1	Y
PIK3R5	Phosphoinositide-3-kinase regulatory subunit 5	*Anolis carolinensis*	XP_016846778.1	N
PIK3R6	Phosphoinositide-3-kinase regulatory subunit 6	*Anolis carolinensis*	XP_016846773.1	Y
PPARGC1A	Peroxisome proliferator-activated receptor gamma coactivator 1-alpha	*Anolis carolinensis*	XP_003221393.1	Y
PPP1R3B	Protein phosphatase 1 regulatory subunit 3B	*Anolis carolinensis*	XP_008114845.1	Y
PPP1R3C	Protein phosphatase 1 regulatory subunit 3C	*Anolis carolinensis*	XP_003223828.1	Y
PPP1R3D	Protein phosphatase 1 regulatory subunit 3D	*Anolis carolinensis*	XP_008108350.1	Y
PRKAA2	5'-AMP-activated protein kinase catalytic subunit α2	*Anolis carolinensis*	XP_003220224.1	Y
PRKCG	Protein kinase C γ type	*Anolis carolinensis*	XP_008116652.1	Y
PTEN	Phosphatase and tensin homolog	*Anolis carolinensis*	XP_003224419.1	Y
PTK2	Protein tyrosine kinase 2	*Anolis carolinensis*	XP_008106513.1	Y
PTPN1	Tyrosine-protein phosphatase non-receptor type 1	*Anolis carolinensis*	XP_003224035.2	Y
RAF1	Proto-oncogene c-RAF	*Anolis carolinensis*	XP_008103430.1	Y
RAPTOR	Regulatory-associated protein of mTOR	*Pogona vitticeps*	XP_020669180.1	Y
RASA1	Ras GTPase-activating protein 1	*Anolis carolinensis*	XP_016846417.1	Y
RHEB	Ras homolog enriched in brain	*Anolis carolinensis*	XP_008110498.1	N
RICTOR	Rapamycin-insensitive companion of mTOR	*Anolis carolinensis*	XP_016851125.1	Y
RIT1	GTP-binding protein Rit1	*Pogona vitticeps*	XP_020652984.1	N
RPS6	Ribosomal protein S6	*Anolis carolinensis*	XP_003216654.1	Y
RPS6KA1	RPS6 kinase α1	*Anolis carolinensis*	XP_003227514.2	N
RPS6KA3	RPS6 kinase α3	*Anolis carolinensis*	XP_016847896.1	Y
RPS6KA4	RPS6 kinase α4	*Anolis carolinensis*	XP_008120908.1	N
RPS6KA5	RPS6 kinase α5	*Python molurus*	XP_007442631.1	N
RPS6KA6	RPS6 kinase α6	*Anolis carolinensis*	XP_008112843.1	Y
RPS6KB1	RPS6 kinase β1	*Anolis carolinensis*	XP_003227314.1	Y

RPS6KB2	RPS6 kinase β2	*Anolis carolinensis*	XP_008109695.1	Y
SFN	Stratifin	*Anolis carolinensis*	XP_003227508.1	Y
SGK1	Serine/threonine-protein kinase	*Anolis carolinensis*	XP_003223340.1	Y
SH2B2	SH2B adapter protein 2	*Pogona vitticeps*	XP_020660655.1	Y
SHC1	SHC adaptor protein 1	*Anolis carolinensis*	XP_016854236.1	Y
SHC2	SHC adaptor protein 2	*Anolis carolinensis*	XP_003229969.1	Y
SHC3	SHC adaptor protein 3	*Anolis carolinensis*	XP_003216492.1	Y
SHC4	SHC adaptor protein 4	*Pogona vitticeps*	XP_020645830.1	Y
SIRT1	Sirtuin 1	*Anolis carolinensis*	XP_003223739.1	Y
SIRT2	Sirtuin 2	*Anolis carolinensis*	XP_003229391.2	Y
SIRT3	Sirtuin 3	*Anolis carolinensis*	XP_003214844.1	Y
SIRT4	Sirtuin 4	*Pogona vitticeps*	XP_020654730.1	Y
SIRT5	Sirtuin 5	*Anolis carolinensis*	XP_003219799.1	Y
SIRT6	Sirtuin 6	*Pogona vitticeps*	XP_020636527.1	Y
SIRT7	Sirtuin 7	*Anolis carolinensis*	XP_008102795.1	Y
SOCS1	Suppressor of cytokine signaling 1	*Python molurus*	XP_007434531.1	Y
SOCS3	Suppressor of cytokine signaling 3	*Anolis carolinensis*	XP_008102404.1	Y
SOCS4	Suppressor of cytokine signaling 4	*Anolis carolinensis*	XP_003225827.1	Y
SOS1	Son of sevenless homolog 1	*Anolis carolinensis*	XP_008120191.2	Y
STK11	Serine/threonine kinase 11	*Anolis carolinensis*	XP_016854140.1	Y
STRADA	STE20-related kinase adaptor alpha	*Anolis carolinensis*	XP_003222425.1	Y
TSC1	Hamartin	*Python molurus*	XP_007425258.1	Y
TSC2	Tuberin	*Anolis carolinensis*	XP_008122202.1	N
ULK2	Unc-51-like kinase 2	*Anolis carolinensis*	XP_016854272.1	Y
ULK3	Unc-51-like kinase 3	*Anolis carolinensis*	XP_003227575.2	Y
YWHAB	14-3-3 protein β/α	*Python molurus*	XP_007426803.1	Y
YWHAE	14-3-3 protein ε	*Anolis carolinensis*	XP_003227508.1	Y
YWHAG	14-3-3 protein γ	*Gekko japonicus*	XP_015263466.1	Y
YWHAQ	14-3-3 protein θ	*Anolis carolinensis*	XP_003215431.1	Y
YWHAZ	14-3-3 protein ζ/δ	*Anolis carolinensis*	XP_003219506.1	Y

Table 1.3: List of genes analyzed in this study with their calculated p-values based on empirical cumulative distribution function of the null data for differences in rate of substitution at each of seven hypothesized transitions in parity mode (see Figure 1.4). P-values are rounded to the nearest thousandth. Significant p-values are indicated in green ($p<0.05$), yellow ($p<0.01$), and red ($p<0.005$).

	Transitions						
Genes	1	2	3	4	5	6	7
AKT1S1	0.538	0.536	0.557	0.522	0.516	0.532	0.510
CALM1	0.011	0.890	0.221	0.091	0.779	0.826	0.008
CCND1	0.296	0.136	0.116	0.151	0.269	0.236	0.236
EIF4E	0.866	0.733	0.724	0.722	0.740	0.745	0.746
EIF4E2	0.281	0.547	0.528	0.508	0.043	0.054	0.641
ELK1	0.176	0.618	0.715	0.300	0.708	0.760	0.299
FOS	0.290	0.127	0.001	0.313	0.725	0.060	0.303
FOXA1	0.522	0.965	0.866	0.979	0.492	0.897	0.199
FOXF1	0.009	0.389	0.808	0.186	0.576	0.479	0.571
FOXJ1	0.252	0.762	0.255	0.216	0.125	0.208	0.325
FOXJ2	0.931	0.069	0.671	0.542	0.021	0.253	0.604
FOXK1	0.029	0.000	0.048	0.324	0.006	0.018	0.036
FOXN2	0.661	0.718	0.607	0.213	0.174	0.027	0.968
FOXN3	0.099	0.094	0.105	0.120	0.089	0.105	0.096
FOXO1	0.283	0.167	0.456	0.074	0.257	0.328	0.317
FOXO3	0.001	0.030	0.002	0.001	0.253	0.001	0.001
FOXO4	0.117	0.059	0.049	0.048	0.717	0.065	0.056
FOXP1	0.179	0.285	0.331	0.283	0.125	0.131	0.137
FOXP4	0.181	0.243	0.219	0.136	0.321	0.248	0.160
GNAI3	0.283	0.291	0.202	0.311	0.307	0.189	0.108
GNB2	0.003	0.588	0.616	0.609	0.757	0.045	0.048
GNB5	0.222	0.641	0.558	0.565	0.279	0.870	0.489
GRAP	0.007	0.325	0.356	0.324	0.635	0.004	0.004
GRB2	0.269	0.234	0.264	0.190	0.289	0.230	0.269
GSK3A	0.178	0.190	0.179	0.177	0.204	0.178	0.179
IGF1	0.445	0.504	0.505	0.478	0.458	0.510	0.586
IGF1R	0.867	0.016	0.005	0.033	0.302	0.012	0.064
IGF2	0.385	0.589	0.600	0.591	0.539	0.470	0.340
IGF2R	0.265	0.267	0.267	0.265	0.264	0.265	0.265
IGFBP1	0.005	0.543	0.462	0.467	0.466	0.503	0.530
IGFBP2	0.661	0.021	0.032	0.012	0.766	0.199	0.448
IGFBP4	0.709	0.042	0.039	0.043	0.979	0.309	0.290
IGFBP5	0.177	0.424	0.316	0.409	0.272	0.326	0.425
IGFBP7	0.419	0.045	0.429	0.645	0.033	0.020	0.026

IKBKB	0.065	0.014	0.005	0.010	0.072	0.004	0.005
INPP5A	0.291	0.342	0.297	0.339	0.346	0.470	0.546
INPPL1	0.155	0.822	0.863	0.719	0.555	0.043	0.236
INSR	0.025	0.909	0.928	0.934	0.849	0.816	0.858
IRS1	0.593	0.002	0.001	0.007	0.133	0.012	0.408
IRS4	0.163	0.028	0.001	0.049	0.335	0.027	0.067
JAK1	0.488	0.355	0.499	0.480	0.282	0.523	0.533
JAK2	0.936	0.010	0.940	0.938	0.932	0.940	0.946
KL	0.009	0.466	0.475	0.521	0.339	0.004	0.004
KRAS	0.480	0.578	0.529	0.611	0.530	0.536	0.524
MAP2K2	0.519	0.351	0.322	0.320	0.321	0.332	0.339
MAP2K3	0.289	0.042	0.042	0.042	0.283	0.304	0.311
MAP2K4	0.282	0.472	0.414	0.426	0.377	0.125	0.386
MAP3K1	0.158	0.254	0.324	0.239	0.966	0.004	0.004
MAP3K10	0.550	0.030	0.025	0.031	0.929	0.787	0.710
MAPK3	0.712	0.473	0.630	0.537	0.141	0.453	0.323
MDM2	0.250	0.187	0.244	0.180	0.208	0.252	0.271
MDM4	0.262	0.647	0.836	0.350	0.374	0.628	0.606
MKNK1	0.713	0.814	0.832	0.720	0.648	0.797	0.807
MLST8	0.075	0.489	0.152	0.807	0.444	0.131	0.058
MRAS	0.297	0.177	0.314	0.120	0.312	0.364	0.401
MTOR	0.606	0.003	0.895	0.812	0.828	0.545	0.572
NRAS	0.284	0.441	0.471	0.491	0.230	0.441	0.176
NRF1	0.044	0.014	0.013	0.013	0.415	0.005	0.005
PDE3B	0.329	0.767	0.271	0.450	0.318	0.325	0.325
PDK1	0.675	0.658	0.645	0.668	0.724	0.472	0.478
PDK2	0.551	0.452	0.598	0.615	0.083	0.003	0.004
PDK3	0.284	0.522	0.281	0.708	0.325	0.393	0.387
PDPK1	0.572	0.784	0.739	0.699	0.072	0.028	0.738
PHKB	0.095	0.035	0.106	0.100	0.016	0.030	0.049
PHKG1	0.133	0.016	0.016	0.016	0.852	0.364	0.377
PIK3CA	0.834	0.061	0.624	0.016	0.864	0.901	0.912
PIK3CB	0.653	0.725	0.742	0.760	0.672	0.274	0.680
PIK3CD	0.903	0.028	0.006	0.018	0.020	0.005	0.005
PIK3CG	0.414	0.103	0.577	0.017	0.775	0.171	0.573
PIK3R1	0.162	0.086	0.135	0.129	0.006	0.199	0.142
PIK3R6	0.003	0.010	0.009	0.009	0.025	0.010	0.011
PPARGC1A	0.566	0.628	0.631	0.697	0.161	0.024	0.608
PPP1R3B	0.083	0.815	0.710	0.659	0.086	0.007	0.007
PPP1R3C	0.343	0.429	0.295	0.177	0.764	0.699	0.429
PPP1R3D	0.732	0.613	0.632	0.607	0.775	0.371	0.408

PRKAA2	0.152	0.192	0.324	0.148	0.164	0.215	0.291
PRKCG	0.374	0.094	0.054	0.138	0.378	0.392	0.392
PTEN	0.318	0.137	0.228	0.096	0.302	0.351	0.197
PTK2	0.018	0.013	0.019	0.011	0.004	0.126	0.012
PTPN1	0.554	0.345	0.311	0.400	0.212	0.450	0.108
RAF1	0.293	0.252	0.338	0.266	0.062	0.022	0.273
RAPTOR	0.154	0.279	0.375	0.393	0.009	0.001	0.001
RASA1	0.526	0.394	0.169	0.421	0.131	0.569	0.607
RICTOR	0.691	0.038	0.008	0.141	0.596	0.012	0.009
RPS6	0.131	0.009	0.131	0.002	0.028	0.002	0.002
RPS6KA3	0.589	0.853	0.608	0.441	0.685	0.270	0.032
RPS6KA6	0.137	0.336	0.358	0.221	0.188	0.333	0.555
RPS6KB1	0.441	0.030	0.564	0.413	0.254	0.585	0.309
RPS6KB2	0.019	0.013	0.024	0.005	0.693	0.002	0.003
SFN	0.154	0.005	0.006	0.005	0.164	0.009	0.063
SGK1	0.491	0.427	0.481	0.464	0.541	0.438	0.476
SH2B2	0.109	0.002	0.002	0.002	0.594	0.632	0.641
SHC1	0.050	0.001	0.001	0.001	0.176	0.983	0.058
SHC2	0.005	0.032	0.005	0.005	0.423	0.004	0.005
SHC3	0.693	0.327	0.407	0.275	0.545	0.772	0.711
SHC4	0.137	0.109	0.073	0.079	0.047	0.058	0.062
SIRT1	0.249	0.006	0.007	0.005	0.849	0.055	0.320
SIRT2	0.026	0.057	0.035	0.035	0.972	0.008	0.004
SIRT3	0.922	0.068	0.870	0.847	0.821	0.928	0.940
SIRT4	0.993	0.005	0.021	0.002	0.093	0.002	0.016
SIRT5	0.456	0.262	0.525	0.060	0.076	0.030	0.031
SIRT6	0.798	0.340	0.438	0.252	0.667	0.070	0.760
SIRT7	0.032	0.009	0.033	0.029	0.016	0.022	0.030
SOCS1	0.338	0.005	0.005	0.005	0.111	0.005	0.044
SOCS3	0.346	0.046	0.956	0.010	0.701	0.585	0.352
SOCS4	0.111	0.005	0.002	0.013	0.658	0.076	0.109
SOS1	0.337	0.134	0.010	0.435	0.113	0.421	0.079
STK11	0.061	0.007	0.007	0.007	0.366	0.704	0.080
STRADA	0.546	0.303	0.518	0.224	0.475	0.695	0.687
TSC1	0.006	0.128	0.111	0.108	0.912	0.375	0.251
ULK2	0.522	0.360	0.513	0.439	0.660	0.245	0.413
ULK3	0.028	0.005	0.004	0.005	0.797	0.016	0.013
YWHAB	0.183	0.362	0.130	0.382	0.361	0.226	0.192
YWHAE	0.178	0.008	0.009	0.007	0.106	0.015	0.100
YWHAG	0.018	0.255	0.067	0.114	0.017	0.001	0.001
YWHAQ	0.151	0.066	0.367	0.066	0.018	0.054	0.145

YWHAZ	0.196	0.128	0.261	0.070	0.153	0.169	0.190

Table 1.4: Number and list of genes with significant ($p<0.05$) rate shifts for each hypothesized transitions, genes with $p<0.005$ in bold.

Transition	No. of Genes	Genes
1	19	CALM1, FOXF1, FOXK1, **FOXO3**, **GNB2**, GRAP, **IGFBP1**, INSR, KL, NRF1, **PIK3R6**, PTK2, RPS6KB2, **SHC2**, SIRT2, SIRT7, TSC1, ULK3, YWHAG
2	36	**FOXK1**, FOXO3, IGF1R, IGFBP2, IGFBP4, IGFBP7, IKBKB, **IRS1**, IRS4, JAK2, MAP2K3, MAP3K10, **MTOR**, NRF1, PHKB, PHKG1, PIK3CD, PIK3R6, PTK2, RICTOR, RPS6, RPS6KB1, RPS6KB2, SFN, **SH2B2**, **SHC1**, SHC2, SIRT1, **SIRT4**, SIRT7, SOCS1, SOCS3, **SOCS4**, STK11, **ULK3**, YWHAE
3	33	**FOS**, FOXK1, **FOXO3**, FOXO4, **IGF1R**, IGFBP2, IGFBP4, IKBKB, **IRS1**, **IRS4**, MAP2K3, MAP3K10, NRF1, PHKG1, PIK3CD, PIK3R6, PTK2, RICTOR, RPS6KB2, SFN, **SH2B2**, **SHC1**, **SHC2**, SIRT1, SIRT2, SIRT4, SIRT7, **SOCS1**, **SOCS4**, SOS1, STK11, **ULK3**, YWHAE
4	33	**FOXO3**, FOXO4, IGF1R, IGFBP2, IGFBP4, IKBKB, IRS1, IRS4, MAP2K3, MAP3K10, NRF1, PHKG1, PIK3CA, PIK3CD, PIK3CG, PIK3R6, PTK2, **RPS6**, RPS6KB2, SFN, **SH2B2**, **SHC1**, SHC2, **SIRT1**, SIRT2, **SIRT4**, SIRT7, **SOCS1**, SOCS3, SOCS4, STK11, **ULK3**, YWHAE
5	15	EIF4E2, FOXJ2, FOXK1, IGFBP7, PHKB, PIK3CD, PIK3R1, PIK3R6, **PTK2**, RAPTOR, RPS6, SHC4, SIRT7, YWHAG, YWHAQ
6	36	FOXK1, FOXN2, **FOXO3**, GNB2, **GRAP**, IGF1R, IGFBP7, **IKBKB**, INPPL1, IRS1, IRS4, **KL**, **MAP3K1**, NRF1, **PDK2**, PDPK1, PHKB, **PIK3CD**, PIK3R6, PPARGC1A, PPP1R3B, RAF1, **RAPTOR**, RICTOR, **RPS6**, **RPS6KB2**, SFN, **SHC2**, SIRT2, **SIRT4**, SIRT5, SIRT7, SOCS1, ULK3, YWHAE, **YWHAG**
7	29	CALM1, FOXK1, **FOXO3**, GNB2, **GRAP**, IGFBP7, IKBKB, **KL**, **MAP3K1**, NRF1, **PDK2**, PHKB, **PIK3CD**, PIK3R6, PPP1R3B, PTK2, **RAPTOR**, RICTOR, **RPS6**, RPS6KA3, **RPS6KB2**, **SHC2**, **SIRT2**, SIRT4, SIRT5, SIRT7, SOCS1, ULK3, **YWHAG**

Table 1.5: Genes with significant ($p<0.05$ and $p<0.005$) rate shifts in multiple clades.

	$p < 0.05$		$p < 0.005$	
Clades	No. of Genes	Genes	No. of Genes	Genes
formosus bicanthalis grammicus	10	PTK2, SHC2, FOXO3, PIK3R6, SIRT7, SIRT2, ULK3, FOXK1, NRF1, RPS6KB2	2	FOXO3, SHC2
formosus grammicus	13	RPS6, SFN, IRS4, PHKB, SOCS1, PIK3CD, IKBKB, IGF1R, RICTOR, IRS1, YWHAE, IGFBP7, SIRT4	2	RSP6, SIRT4
bicanthalis grammicus	5	KL, GRAP, YWHAG, GNB2, CALM1		
formosus	19	SHC1, MAP2K3, MTOR, FOS, MAP3K10, JAK2, IGFBP4, SOS1, FOXO4, SH2B2, STK11, SOCS4, PIK3CG, SIRT1, SOCS3, IGFBP2, PIK3CA, RPS6KB1, PHKG1	12	SHC1, SOCS4, SOCS1, MTOR, ULK3, FOS, SH2B2, SIRT1, FOXK1, IGF1R, IRS1, IRS4
bicanthalis	4	FOXF1, IGFBP1, TSC1, INSR	3	IGFBP1, GNB2, PIK3R6
grammicus	16	MAP3K1, PIK3R1, PPARGC1A, YWHAQ, PDPK1, INPPL1, PDK2, EIF4E2, RAF1, RPS6KA3, FOXJ2, FOXN2, SHC4, SIRT5, PPP1R3B, RAPTOR	11	SIRT2, PIK3CD, MAP3K1, KL, PTK2, GRAP, IKBKB, YWHAG, RAPTOR, PDK2, RPS6KB2

Table 1.6: Genes with significant ($p<0.05$) rate shifts at multiple transitions. Groups of branches not represented did not share any genes with shifts in rate of evolution.

Transitions	No. of Genes	Genes
1 2 3 4 5 6 7	2	PIK3R6, SIRT7
1 2 3 4 5 7	1	PTK2
1 2 3 4 6 7	5	SHC2, FOXO3, ULK3, NRF1, RPS6KB2
1 2 3 5 6 7	1	FOXK1
2 3 4 5 6 7	1	PIK3CD
1 3 4 6 7	1	SIRT2
2 3 4 6 7	3	SOCS1, IKBKB, SIRT4
2 4 5 6 7	1	RPS6
1 5 6 7	1	YWHAG
2 3 4 6	5	SFN, IRS4, IGF1R, IRS1, YWHAE
2 3 6 7	1	RICTOR
2 5 6 7	2	PHKB, IGFBP7
1 6 7	3	KL, GRAP, GNB2
2 3 4	10	SHC1, MAP2K3, MAP3K10, IGFBP4, SH2B2, STK11, SOCS4, SIRT1, IGFBP2, PHKG1
5 6 7	1	RAPTOR
1 7	1	CALM1
2 4	1	SOCS3
3 4	1	FOXO4
6 7	4	MAP3K1, PDK2, SIRT5, PPP1R3B
1	4	FOXF1, IGFBP1, TSC1, INSR
2	3	MTOR, JAK2, RPS6KB1
3	2	FOS, SOS1
4	2	PIK3CG, PIK3CA
5	5	PIK3R1, YWHAQ, EIF4E2, FOXJ2, SHC4
6	5	PPARGC1A, PDPK1, INPPL1, RAF1, FOXN2
7	1	RPS6KA3

Table 1.7: Number and list of genes with significant ($p<0.05$) evidence of positive selection in the branch-site test at each hypothesized transition (Fig. 1.#). Genes in bold have sites that were specifically identified to be under positive selection.

Transition	No. of Genes	Genes
1	4	GNB2, **PHKB**, PIK3R6, ULK3
2	14	**FOXP1**, GNB2, GRAP, **IGFBP4**, MKNK1, PHKB, PIK3R1, **PIK3R6**, PRKCG, **RAF1**, RICTOR, SHC3, SIRT3, ULK2
3	0	
4	4	GRB2, **IGFBP2**, IGFBP7, INPPL1
5	6	IGFBP1, PHKB, PRKAA2, RAF1, RASA1, SHC1
6	2	GNB2, GRB2
7	7	IGF2R, PHKB, PRKAA2, RAF1, RPS6KA6, SHC1, TSC1

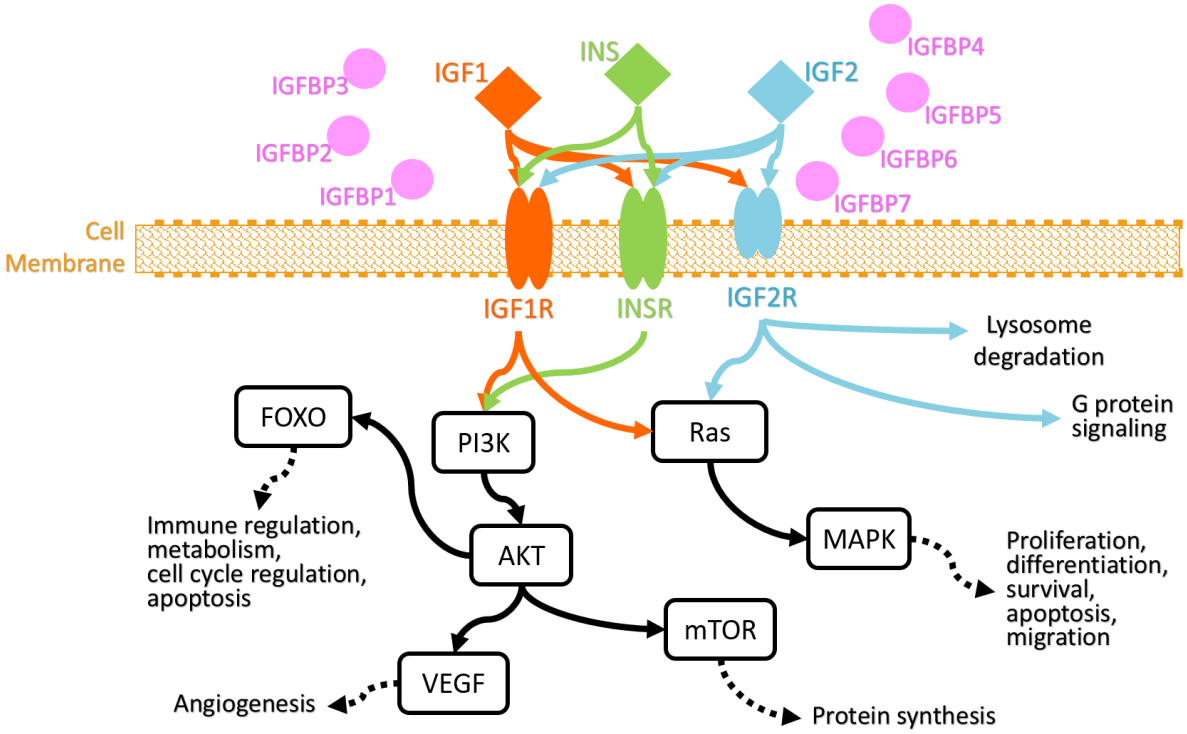

Figure 1.1: A highly simplified depiction of regulatory pathways activated by the insulin and insulin-like signaling network.

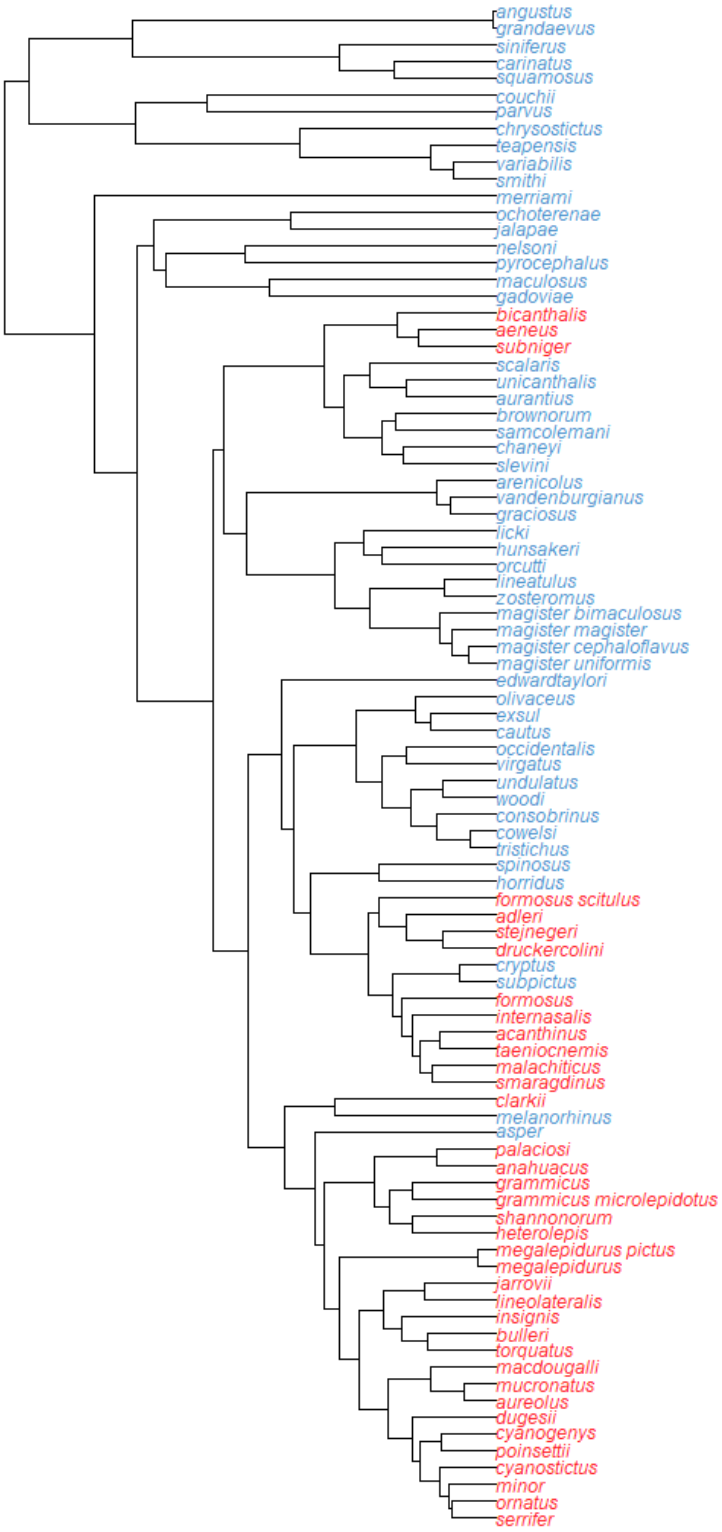

Figure 1.2: Phylogeny of *Sceloporus* species from Leaché et al. (2016). Oviparous species names are indicated in blue and viviparous in red.

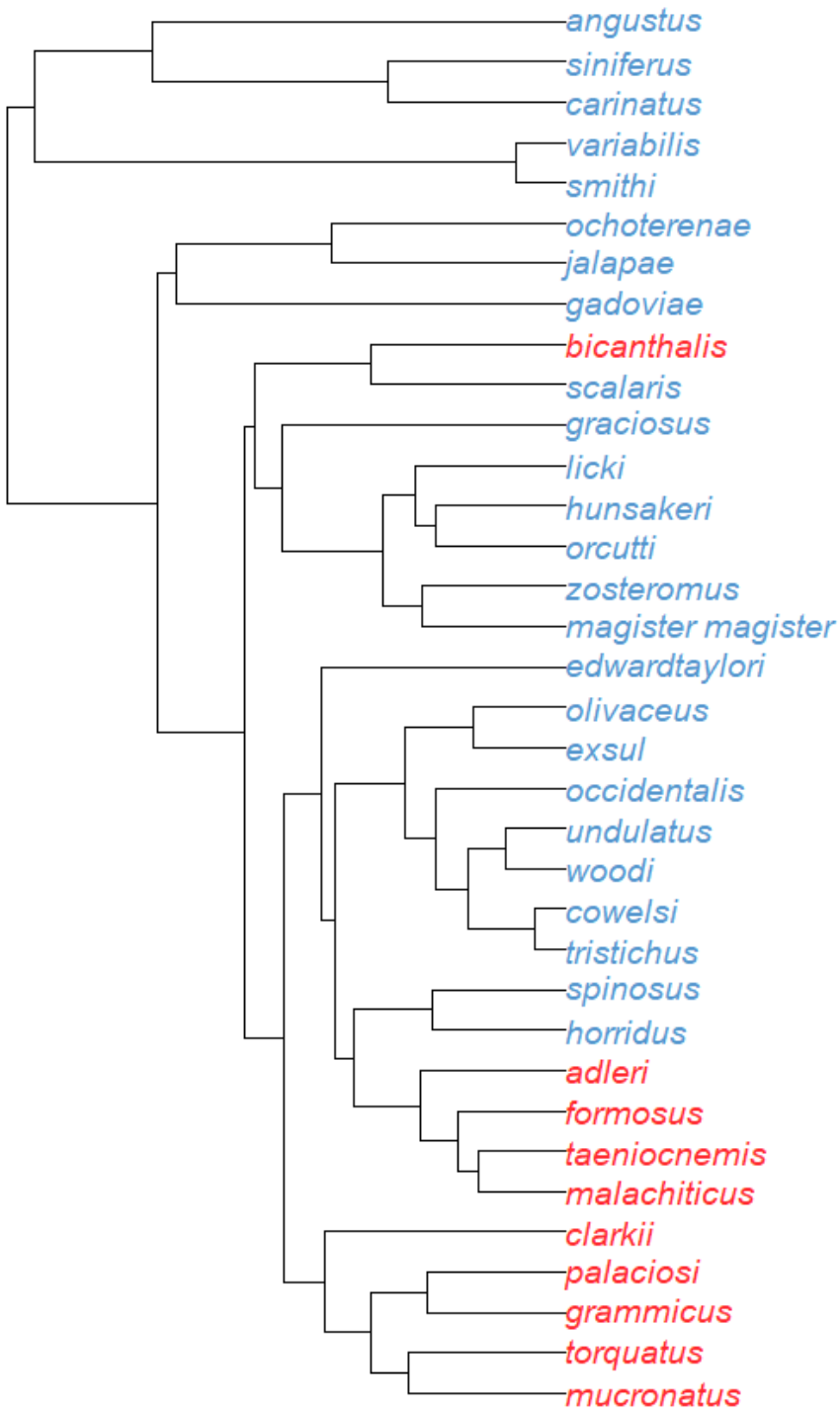

Figure 1.3: Reduced phylogeny of *Sceloporus* species used to calculate rate shift changes of IIS network genes in viviparous clades.

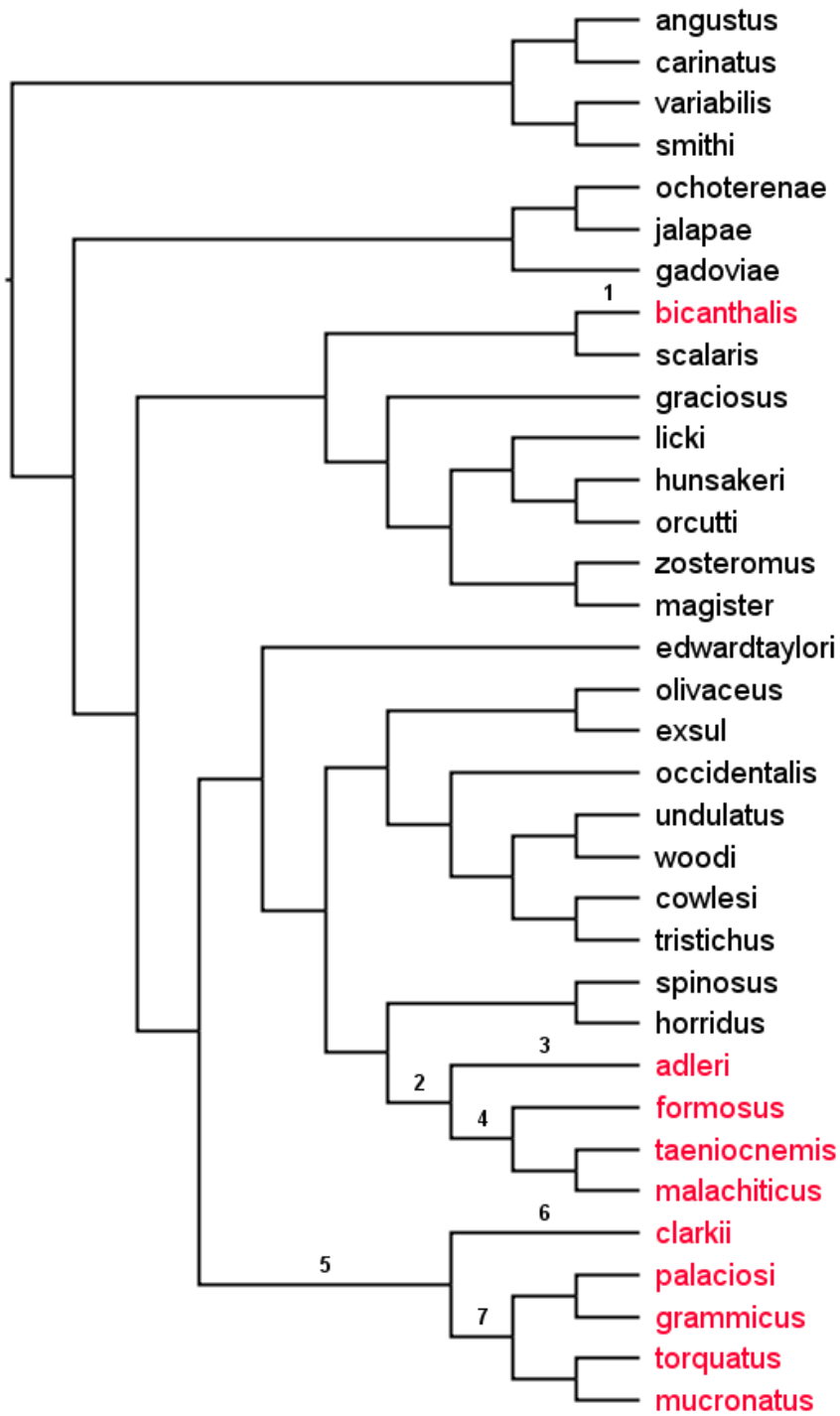

Figure 1.4: Cladogram of *Sceloporus* species used in rate shift and positive selection analyses. Viviparous species are indicated in red. Each branch label (1-7) indicates a branch with a hypothesized transition, used as foreground branches in PAML, predicted from stochastic character mapping. Clades of viviparous species are labeled for comparison by a representative species: *bicanthalis* (1), *formosus* (2-4), and *grammicus* (5-7).

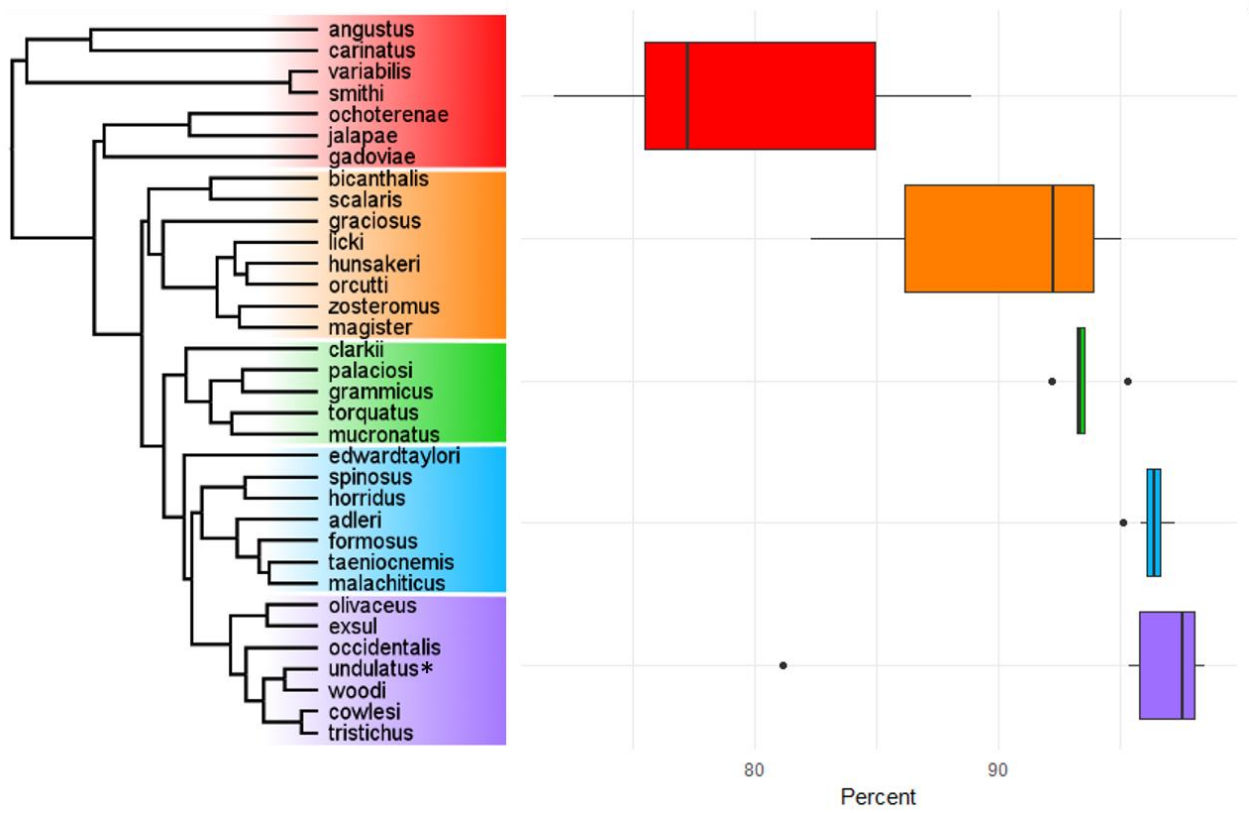

Figure 1.5: Phylogeny and boxplot with percentage of mapped reads to an *S. undulatus* reference. Colors represent groups of species groups which are created based on phylogenetics, karyotypes, and traditional systematics in the genus. The star designates the reference genome species, *S. undulatus*. Two groups are polyphyletic: red and teal. However, the placement of ancestrally diverged groups in the red group are still uncertain, and they sometimes group monophyletically. In the teal group, *S. edwardtaylori* also groups polyphyletically; however, *S. edwardtaylori*, *S. spinosus*, and *S. horridus* are still labeled as a species group together. Outliers are: *S. exsul*, purple, 81.13%; *S. adleri*, teal, 95.16%; *S. mucronatus*, green, 95.30%; and *S. palaciosi*, green, 92.24%.

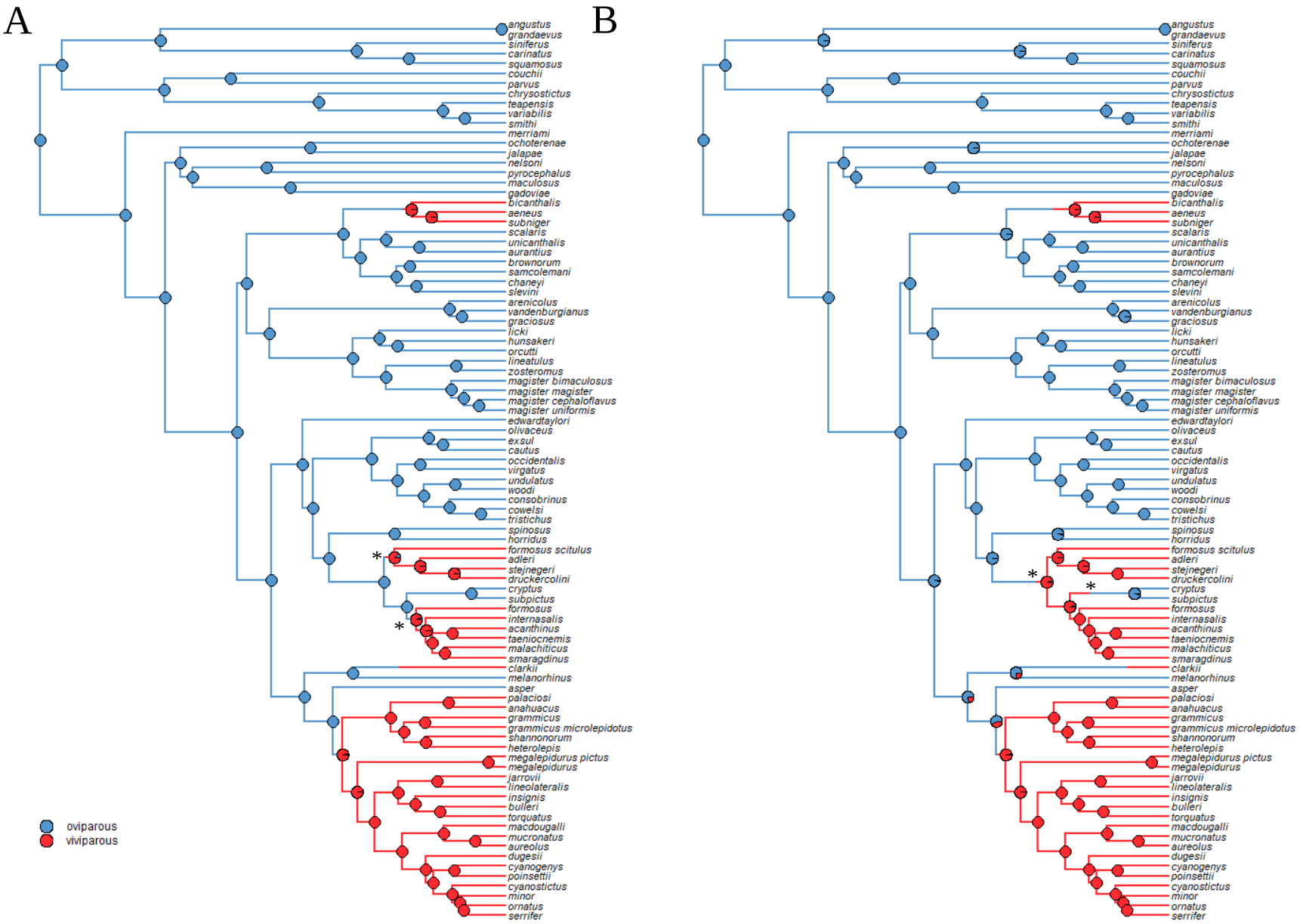
A
B
angustus
grandaevus
siniferus
carinatus
squamosus
couchii
parvus
chrysostictus
teapensis
variabilis
smithi
merriami
ochoterenae
jalapae
nelsoni
pyrocephalus
maculosus
gadoviae
bicanthalis
aeneus
subniger
scalaris
unicanthalis
aurantius
brownorum
samcolemani
chaneyi
slevini
arenicolus
vandenburgianus
graciosus
licki
hunsakeri
orcutti
lineatulus
zosteromus
magister bimaculosus
magister magister
magister cephaloflavus
magister uniformis
edwardtaylori
olivaceus
exsul
cautus
occidentalis
virgatus
undulatus
woodi
consobrinus
cowelsi
tristichus
spinosus
horridus
formosus scitulus
adleri
stejnegeri
druckercolini
cryptus
subpictus
formosus
internasalis
acanthinus
taeniocnemis
malachiticus
smaragdinus
clarkii
melanorhinus
asper
palaciosi
anahuacus
grammicus
grammicus microlepidotus
shannonorum
heterolepis
megalepidurus pictus
megalepidurus
jarrovii
lineolateralis
insignis
bulleri
torquatus
macdougalli
mucronatus
aureolus
dugesii
cyanogenys
poinsettii
cyanostictus
minor
ornatus
serrifer
oviparous
viviparous

Figure 1.6: Ancestral state reconstruction of viviparity evolution in *Sceloporus* under models in which reversions to oviparity are (A) impossible or (B) unlikely. The proportion of circles in each color indicates probability of that parity mode at that node from simulations. Primary differences in where transitions are most probably occurring in major viviparous radiations are highlighted by asterisks (*).

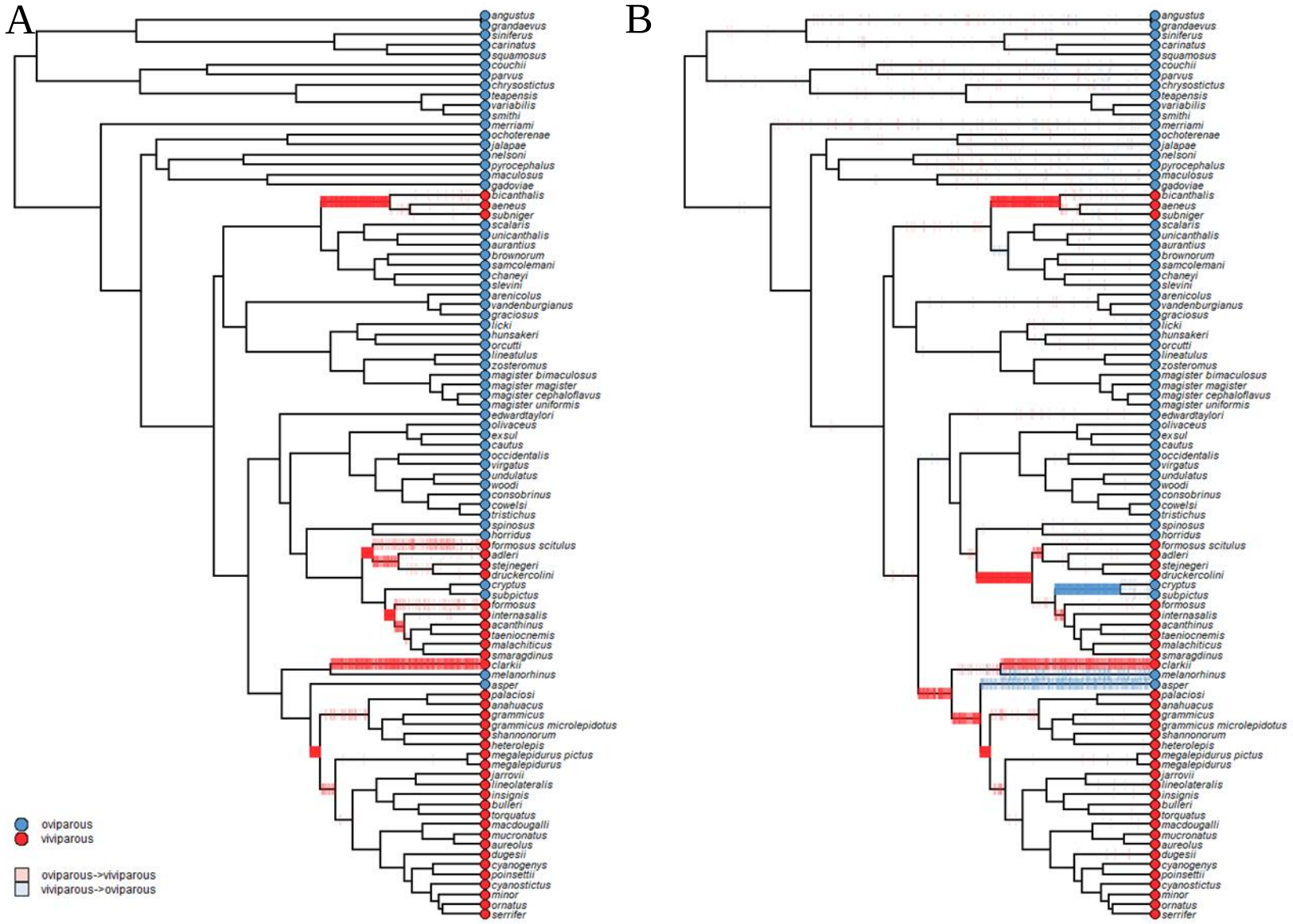
A
B
angustus
grandaevus
siniferus
carinatus
squamosus
couchii
parvus
chrysostictus
teapensis
variabilis
smithi
merriami
ochoterenae
jalapae
nelsoni
pyrocephalus
maculosus
gadoviae
bicanthalis
aeneus
subniger
scalaris
unicanthalis
aurantius
brownorum
samcolemani
chaneyi
slevini
arenicolus
vandenburgianus
graciosus
licki
hunsakeri
orcutti
lineatulus
zosteromus
magister bimaculosus
magister magister
magister cephaloflavus
magister uniformis
edwardtaylori
olivaceus
exsul
cautus
occidentalis
virgatus
undulatus
woodi
consobrinus
cowelsi
tristichus
spinosus
horridus
formosus scitulus
adleri
stejnegeri
druckercolini
cryptus
subpictus
formosus
internasalis
acanthinus
taeniocnemis
malachiticus
smaragdinus
clarkii
melanorhinus
asper
palaciosi
anahuacus
grammicus
grammicus microlepidotus
shannonorum
heterolepis
megalepidurus pictus
megalepidurus
jarrovii
lineolateralis
insignis
bulleri
torquatus
macdougalli
mucronatus
aureolus
dugesii
cyanogenys
poinsettii
cyanostictus
minor
ornatus
serrifer
oviparous
viviparous
oviparous->viviparous
viviparous->oviparous

Figure 1.7: Mapping of predicted transitions of each posterior sample under two models of viviparity evolution in *Sceloporus*, (A) transitions back to oviparity are impossible and (B) transitions back are unlikely. Density of color on a branch indicates probability of a transition along that branch.

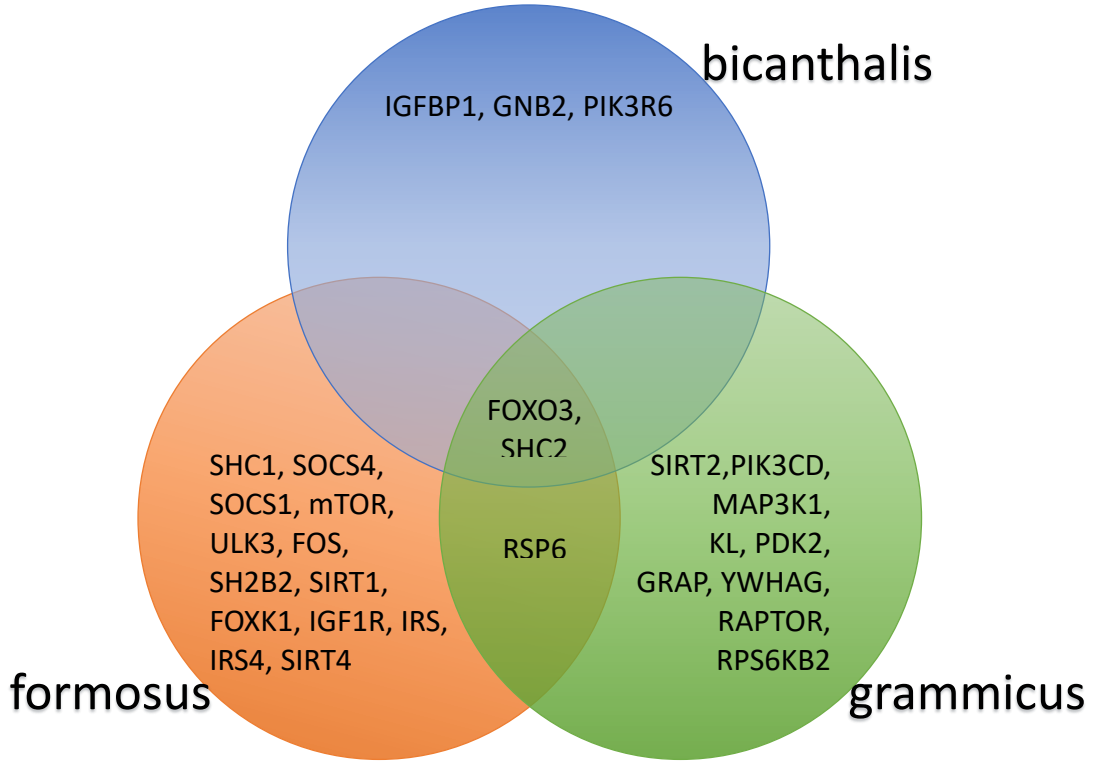

Figure 1.8: Venn diagram showing genes with significant ($p<0.005$) increases in rate in each group of viviparous *Sceloporus* groups.

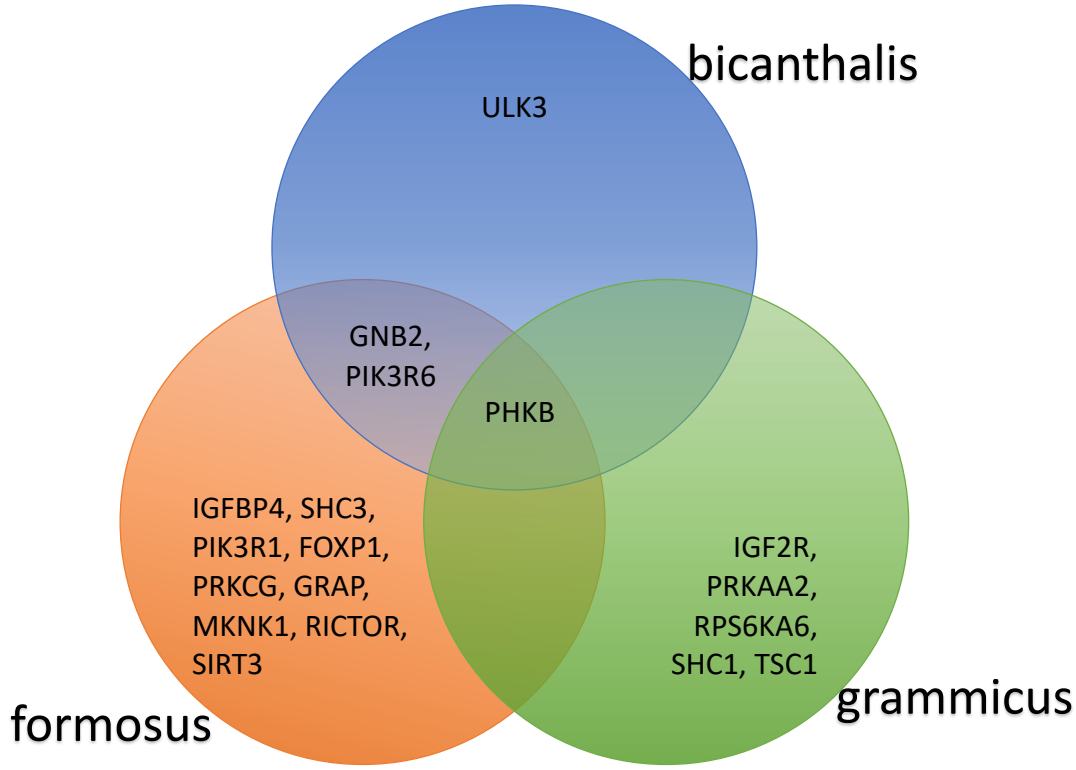

Figure 1.9: Venn diagram showing genes with significant ($p<0.05$) support for positive selection at the branch preceding each group of viviparous *Sceloporus* groups.